AD-A031 293 MASSACHUSETTS INST OF TECH CAMBRIDGE DEPT OF OCEAN E--ETC F/G 13/10
DETERMINATION OF DAMPING COEFFICIENTS OF SWATH CATAMARAN USING --ETC(U)
JAN 75 K KIM N00014-67-A-0204-0023
UNCLASSIFIED 75-4 NL

1 OF 1
ADA031293

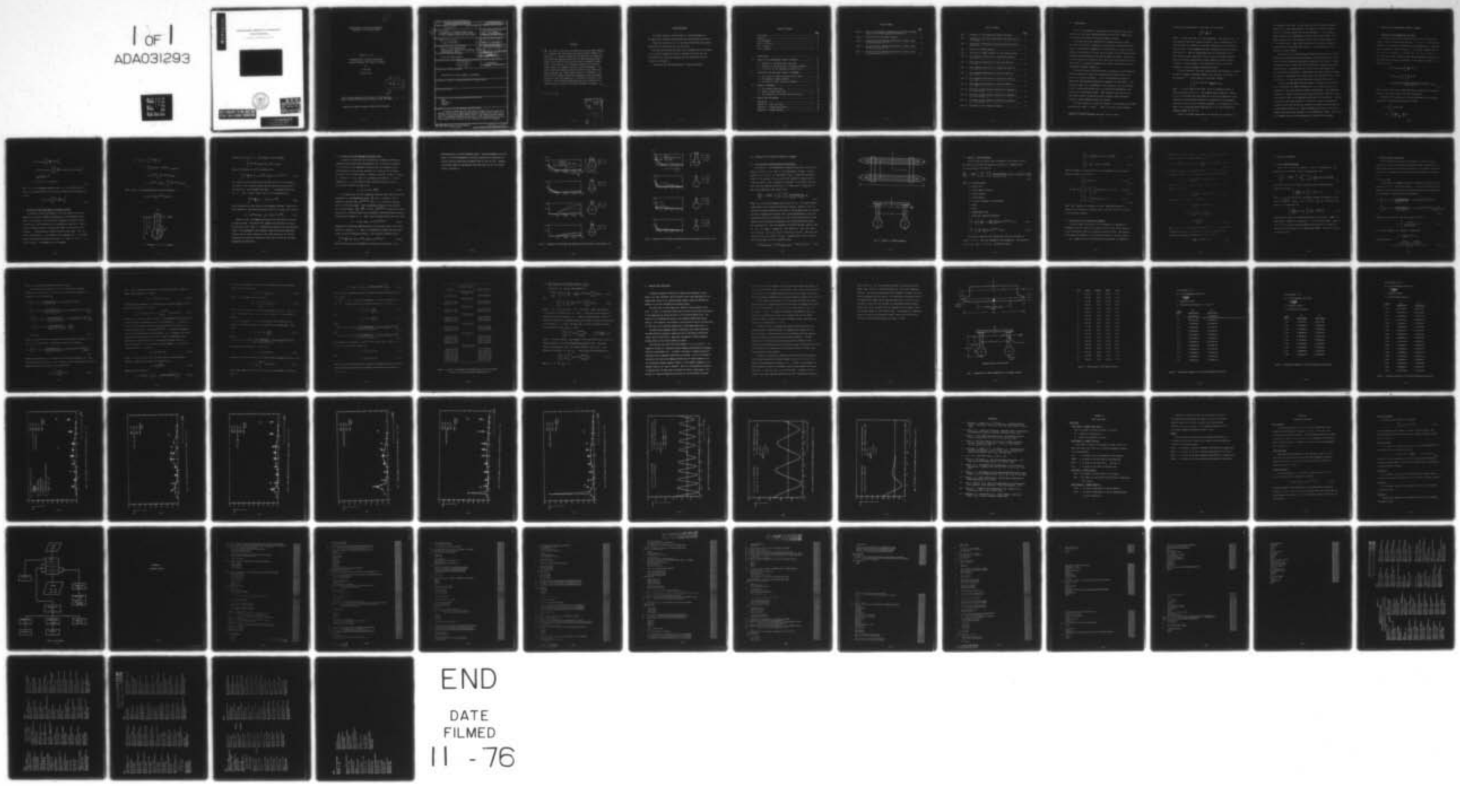

END
DATE
FILMED
11 - 76

1

MASSACHUSETTS INSTITUTE OF TECHNOLOGY
Department of Ocean Engineering

Report No. 75-4

DETERMINATION OF DAMPING COEFFICIENTS OF SWATH CATAMARAN USING THIN SHIP THEORY

by

Ki-Han Kim

January 1975

This work was supported by the Office of Naval Research, Contract N00014-67-A-0204-0023, NR 062-411, MIT OSP 70808. 220039

Approved for public release; distribution unlimited.

REPORT DOCUMENTATION PAGE		READ INSTRUCTIONS BEFORE COMPLETING FORM
1. REPORT NUMBER (14) 75-4	2. GOVT ACCESSION NO.	3. RECIPIENT'S CATALOG NUMBER
4. TITLE (and Subtitle) (6) DETERMINATION OF DAMPING COEFFICIENTS OF SWATH CATAMARAN USING THIN SHIP THEORY,		5. TYPE OF REPORT & PERIOD COVERED (9) Final Report.
		6. PERFORMING ORG. REPORT NUMBER
7. AUTHOR(s) (10) Ki-Han Kim		8. CONTRACT OR GRANT NUMBER(s) (15) N00014-67-A-0204-0023
9. PERFORMING ORGANIZATION NAME AND ADDRESS Dept. of Ocean Engineering Massachusetts Institute of Technology Cambridge, Ma 02139		10. PROGRAM ELEMENT, PROJECT, TASK AREA & WORK UNIT NUMBERS (16) NR-062-411 MIT-OSP-70808
11. CONTROLLING OFFICE NAME AND ADDRESS Office of Naval Research		12. REPORT DATE (11) January 1975
		13. NUMBER OF PAGES 65
14. MONITORING AGENCY NAME & ADDRESS(if different from Controlling Office) (12) 71p.		15. SECURITY CLASS. (of this report) Unclassified
		15a. DECLASSIFICATION/DOWNGRADING SCHEDULE

16. DISTRIBUTION STATEMENT (of this Report)

Distribution of this document is unlimited.

17. DISTRIBUTION STATEMENT (of the abstract entered in Block 20, if different from Report)

18. SUPPLEMENTARY NOTES

19. KEY WORDS (Continue on reverse side if necessary and identify by block number)

SWATH
Ship Motion
Damping

20. ABSTRACT (Continue on reverse side if necessary and identify by block number)

A computer program has been developed to compute the pitch and heave damping coefficients of SWATH including forward speed effects based on the thin ship theory developed by Newman (1959). The results include comparisons of the damping coefficients with Lee's (1974) experiments for several Froude numbers and the effect of hull distance variations on damping.

ABSTRACT

This report deals with the problem of pitch and heave damping of a catamaran with small-waterplane-area-twin-hull (SWATH) configuration. A computer program has been developed to compute the pitch and heave damping coefficients of SWATH including forward speed effects based on the thin ship theory developed by Newman (1959). Calculations of the damping coefficients for several Froude numbers are compared with Lee's (1974) experiments. The results show that damping is greatly affected by the Brard parameter, $\omega V/g$ when the forward speed effects are considered. The effect of hull distance variation on damping is also considered. The results show that damping is an oscillatory function of hull distance. The oscillatory phenomenon dies out as the hull distance increases, and also as the Brard parameter increases.

(omega)(V)/g,

ACKNOWLEDGEMENTS

The author wishes to thank Professor J. Nicholas Newman for initiating this research and constantly give his guidance and advice.

Thanks are also due to Dr. K. June Bai without whose encouraging assistance this work would not have been done.

The author's gratitude also goes to Dr. Choung M. Lee of the NSRDC for his helpful suggestions and for providing the author with the experimental data which are compared with the theoretical results in Figures 6 through 11.

Discussions with Professor Ronald W. Yeung were helpful.

TABLE OF CONTENTS

LIST OF TABLES

LIST OF FIGURES

I. INTRODUCTION

Due to the advantages of large deck area and stable motion characteristics in heavy seas, small-waterplane-area-twin-hull (SWATH) type of catamaran has become an interesting subject recently.

In recent work on the prediction of catamaran motions in waves, Lee (Pien and Lee [11][1]) extended the strip-theory to catamaran configurations. A fundamental assumption in the strip-theory is that the hydrodynamic characteristics of a ship can be inferred from the two-dimensional stripwise characteristics of each section along the length. The effects of forward speed are included in Lee's work by the strip-theory synthesis rather than by a rigorous introduction of forward speed effects into the hydrodynamic boundary conditions.

The results based on the strip-theory are generally in good agreement with the experiments, except for a pronounced resonance effect in the theory at a critical frequency. At the corresponding wavelength the motions are substantially overpredicted compared with experiments. This resonance seems to be a consequence of the presence of near-zero damping at zero forward speed and the use of the zero-speed hydrodynamic coefficients in a strip-theory manner. This problem occurs only for hull forms where bulbous cylindrical sections, having a small waterplane area and a large submerged volume, are dominant.

To be more specific, let us first consider a two-dimensional thin-body section with a shape $y = \pm h(z)$. Then it is known that the damping

[1]Numbers in brackets designate Reference at end of paper.

coefficient is proportional to the square of the integral

$$\int_{-T}^{0} e^{Kz} \frac{dh}{dz} dz$$

where T is the draft and K is the wavenumber. (See Section 2.1). It seems apparent that for a bulbous form where dh/dz changes sign, the above integral will vanish for a suitable combination of the wavenumber and hull shape. This phenomenon has been investigated earlier by Motora and Koyama [7]. They did experimental work on two-dimensional wave-excitationless forms, which have similar forms to the SWATH demi-hull. Frank [4] did some computations on heave damping for various bulbous cylinders. In both studies, it was shown that there is a critical frequency at which the damping coefficients vanish.

In three dimensions with zero forward speed, the situation is changed because the damping coefficient depends on an integral, with respect to the waveangle θ, of the square of the surface integral

$$\int_{-L}^{L} \int_{-T}^{0} e^{Kz + iKx \cos\theta} \frac{\partial h(x,z)}{\partial z} dz\, dx$$

where L is half length of the body. Since the damping integral is positive-definite for all θ, zero-damping seems impossible. However, it can be anticipated that there might occur near-zero damping for long cylindrical vessels having essentially the appropriate two-dimensional form because there will be a dominant waveangle $\frac{\pi}{2}$ as suggested by strip theory or the stationary phase approximation of the three-dimensional damping integral for $KL >> 1$.

Finally, if forward speed effects are included, the possibility of

zero damping is even less. In this case, the three-dimensional damping coefficient is again proportional to the square of a surface integral similar to that shown above, but now the wavenumber K is no longer a single constant, but, depending on the value of the Brard number $\omega V/g$, takes on either two or four discrete values, each of which depends on θ (See Newman [8]). Thus, since the square of the surface integral is integrated over a continuous spectrum of K, the probability of zero damping is greatly reduced.

Calculation of the three-dimensional damping coefficients, including forward speed effects without the assumption of strip theory is so complicated that some alternative simplifying assumptions are required. Newman [8] presented such a theory for "thin" mono-hulls, including illustrative calculations for a mathematical hull form for which experimental data had been obtained by Golovato. Subsequently, Gerritsma, Kerwin and Newman [5] presented comparisons of the same theory with experiments for a Series 60 hull form. In both cases the comparison was qualitatively useful.

In this report,Newman's thin-ship theory is applied to the catamaran hulls, especially with SWATH configuration, in an attempt to avoid the deficiency of the strip theory at nonzero forward speed. The fundamental assumption of Newman's thin-ship theory may be valid for these hull forms, since they are thin in the important region near the free surface. Moreover, to extend the practical validity of the present results, the submerged cylindrical hull portion will be treated by a modified thin-ship approach as described in Section 2.3. Based on Newman's work [8], pitch and heave damping coefficients are calculated for the NSRDC Model MODCAT. The results are compared with Lee's [6] experiments for various Froude numbers.

II. DAMPING OF TWO-DIMENSIONAL BULBOUS CYLINDERS

2.1 Damping of a Two-Dimensional Thin Body

Consider a thin vertical body which is in an oscillatory heave motion on the free surface with velocity $\dot{\zeta} = V \cos \omega t$. The fluid is assumed to be inviscid, irrotational and of infinite depth. Assume the body is symmetrical about the z-axis, z is positive upwards and its hull function is given by $y = \pm h(z)$ for $-T \leq z \leq 0$, where T is the draft of the body. Then the velocity potential which satisfies the the linearized free surface condition, in the region of positive y , is known to be [10]:

$$\phi = 2e^{Kz} V \sin(Ky-\omega t) \int_{-T}^{0} \frac{dh}{d\zeta} e^{K\zeta} d\zeta$$

$$- \frac{2}{\pi} V \cos \omega t \int_{0}^{\infty} \int_{-T}^{0} \frac{dh}{d\zeta} e^{-ky}$$

$$\cdot \frac{(k \cos kz + K \sin kz)\ (k \cos k\zeta + K \sin k\zeta)}{k(k^2 + K^2)} d\zeta\, dk \tag{2.1}$$

where the first term on the right hand side is related to the outgoing waves and the second term, to the local disturbance.

From Bernoulli's equation, the total hydrodynamic force acting on the body in z-direction is obtained as follows:

$$Z = 2 \int_{-T}^{0} p \cos(n,z)\, ds$$

$$\cong - 2 \int_{-T}^{0} \left(\frac{\partial\phi}{\partial t}\right)_{y=0} \frac{dh}{dz} dz$$

$$= 4\omega\rho \; V \cos \omega t \left[\int_{-T}^{0} \frac{dh}{dz} \, e^{Kz} \, dz \right]^2$$

$$- \frac{4}{\pi} \omega\rho \; V \sin \omega t \int_{0}^{\infty} \left[\int_{-T}^{0} \frac{dh}{dz} \, (k \cos kz + K \sin kz) dz \right]^2$$

$$\cdot \frac{1}{k(k^2 + k^2)} \, dk$$

$$\equiv b_{33} \; V \cos \omega t - a_{33} \; V\omega \sin \omega t \tag{2.2}$$

where b_{33} is the damping coefficient and a_{33} is the added mass coefficient. From the relation (2.2) we have a formula for the damping coefficient:

$$b_{33} = 4\omega\rho \left[\int_{-T}^{0} e^{Kz} \frac{dh}{dz} \, dz \right]^2 \tag{2.3}$$

2.2 Extension of Thin Ship Result to Bulbous Cylinder

As a means to check the validity of thin ship theory to find the damping coefficients of SWATH configurations, a two-dimensional model (Fig.1) is considered. In this section, damping of a heaving circular cylinder with a thin vertical strut is examined by using (2.3). Define a polar coordinate system (r,θ) with the origin at the center of the cylinder, θ being positive clockwise starting from z-axis. Let $h(z)$ be the hull function, r_0 the radius of the cylinder, and θ_0 the angle between z-axis and the bottom of the strut. If $dh/dz = 0$ for $z > -T + r_0(1 + \cos\theta_0)$, the integral in (2.3) becomes:

$$\int_{-T}^{0} e^{Kz} \frac{dh}{dz} dz = \int_{-T}^{-H} e^{Kz} \frac{dh}{dz} dz$$

$$= \int_{\pi}^{\theta_0} e^{Kr_0 \cos\theta - K(T-r_0)} r_0 \cos\theta \, d\theta$$

$$= - r_0 e^{-KT_0} \int_{\theta_0}^{\pi} e^{Kr_0 \cos\theta} \cos\theta \, d\theta$$

$$= - r_0 e^{-KT_0} \{\pi I_1(Kr_0) - \int_{0}^{\theta_0} e^{Kr_0 \cos\theta} \cos\theta \, d\theta\} \tag{2.4}$$

where $I_1(z)$ is the modified Bessel function defined by

$$I_1(z) = \frac{1}{\pi} \int_{0}^{\pi} e^{z \cos\theta} \cos\theta \, d\theta \quad .$$

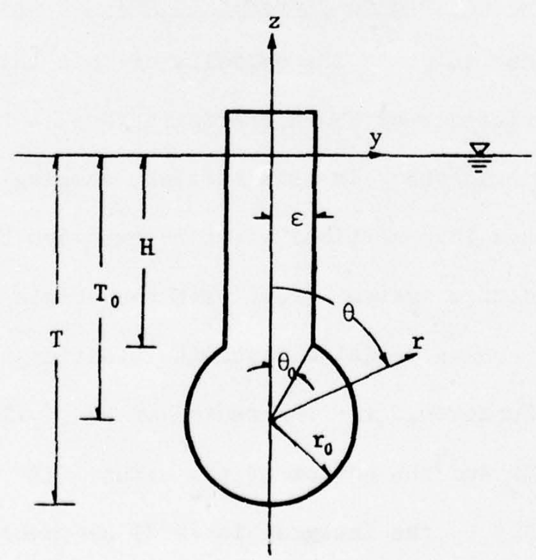

Fig. 1 Geometry of Bulbous Cylinder

Assuming $Kr_0 \sin\theta_0 << 1$, the integral in (2.4) becomes:

$$\int_0^{\theta_0} e^{Kr_0\cos\theta} \cos\theta \, d\theta \cong \theta_0 \, e^{Kr_0} + O(\theta_0{}^2) \quad .$$

Hence, the integral in (2.3) is reduced to be:

$$\int_{-T}^{0} e^{Kz} \frac{dh}{dz} dz \cong - \pi r_0 \, e^{-KT_0} \, I_1(Kr_0) + \varepsilon \, e^{-K(T_0-r_0)} \quad . \tag{2.5}$$

In a sense, the first term on the right hand side of (2.5) represents the effect of the circular cylinder and the second term, the effect of the thin strut. As an extreme case where ε is negligibly small and $Kr_0 \to 0$, then $I_1(Kr_0) \sim \frac{1}{2} Kr_0$ and (2.5) is approximated by:

$$\int_{-T}^{0} e^{Kz} \frac{dh}{dz} dz \sim -\frac{1}{2} \pi r_0{}^2 K e^{-KT_0} \tag{2.6}$$

which represents only the effect of the submerged cylinder. Then the far field behavior of the velocity potential from (2.1), using (2.6), becomes:

$$\phi \sim 2V e^{Kz} \sin (Ky - \omega t) \, (-\frac{1}{2} \pi r_0{}^2 K e^{-KT_0}) \tag{2.7}$$

Based on (2.5), the damping coefficients are calculated for several cylindrical forms. The results are compared with Frank's [4] in Fig. 2 and with Lee's [6] in Fig. 3. Agreements are good for only low frequency range. Poor agreements in the frequency range of practical importance indicate that we need to modify the thin ship results for the circular cylindrical part which is actually not thin and for which the thin ship assumption may break down.

2.3 Correction for the Submerged Cylindrical Part

In order to account for the discrepancies in damping coefficients resulting from the thin ship approximation, Eqn. (2.5) will be modified for the effect of the submerged cylindrical part by comparing the far field behavior of the velocity potential (2.7) with that of the known solution of the circular cylinder. Consider a circular cylinder of radius r_0 located at $z = -T_0$ which is oscillating with velocity $\dot{\zeta} = V\cos\omega t$. Assuming $T_0 >> r_0$ and using the same coordinate system as in Fig. 1, the velocity potential is known to be:

$$\phi = -V\, r_0^{\,2} \cos\omega t \,\frac{\cos\,\theta}{r} \tag{2.8}$$

It is known (e.g. (13.31) in Wehausen & Laitone [13]) that the velocity potential of a two-dimensional source $\frac{Q}{2\pi}\log r$ located at $(0,-\zeta)$ behaves at infinity like $Qe^{K(z+\zeta+iy)}$ where Q is the source strength and K is the wave number. The corresponding behavior of the potential of a vertical dipole $\frac{Q}{2\pi}\frac{\cos\theta}{r}$ will be $QKe^{K(z+\zeta+iy)}$ since the velocity potential of a vertical dipole can be obtained by differentiating the source potential with respect to ζ . Then it can be readily shown from (2.8) that:

$$\phi \sim -V\, r_0^{\,2} \cos\omega t \cdot 2\pi\, K\, e^{K(z-T_0+iy)} \tag{2.9}$$

Comparing (2.9) with the limiting case of the thin ship result (2.7), they differ by a factor of 2 . Thus it is reasonable to modify the thin ship results (2.5) by doubling the effect of the circular cylindrical part:

$$\int_{-T}^{0} e^{Kz}\,\frac{dh}{dz}\,dz \cong -2\pi\, r_0\, e^{-KT_0}\, I_1(Kr_0) + \varepsilon e^{-K(T_0-r_0)} \tag{2.10}$$

Note that the last term is unmodified reflecting the importance of the

waterplane area in the low frequency limit. The same arguments will also apply to the three-dimensional case when we perform the integration of the hull function which has the similar form to that in (2.5). Damping coefficients based on the modified thin ship result (2.10) are plotted in Fig. 2 and Fig. 3.

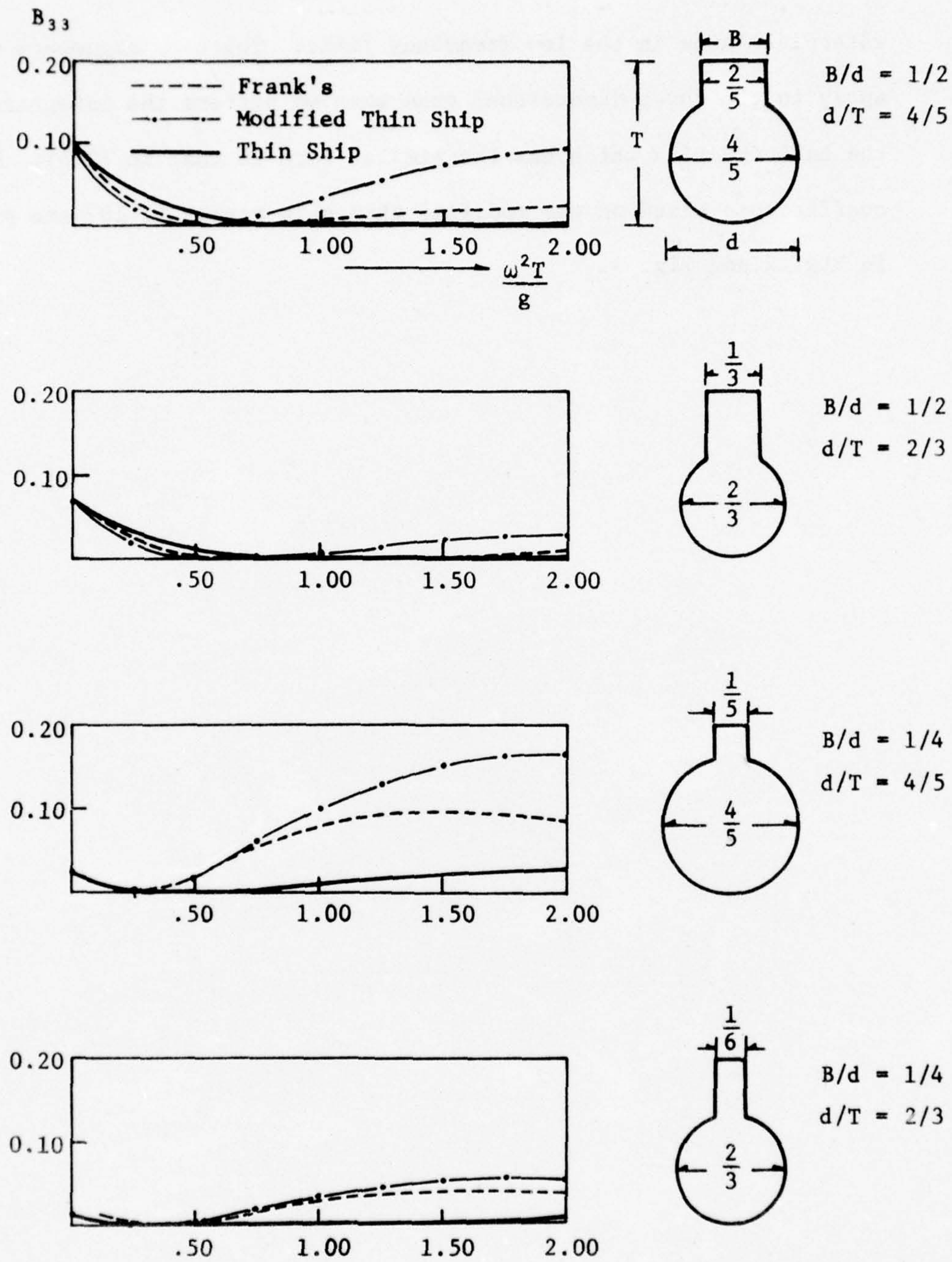

Fig. 2 Comparison of Thin-Ship and Modified Thin-Ship Results with Frank's [4]

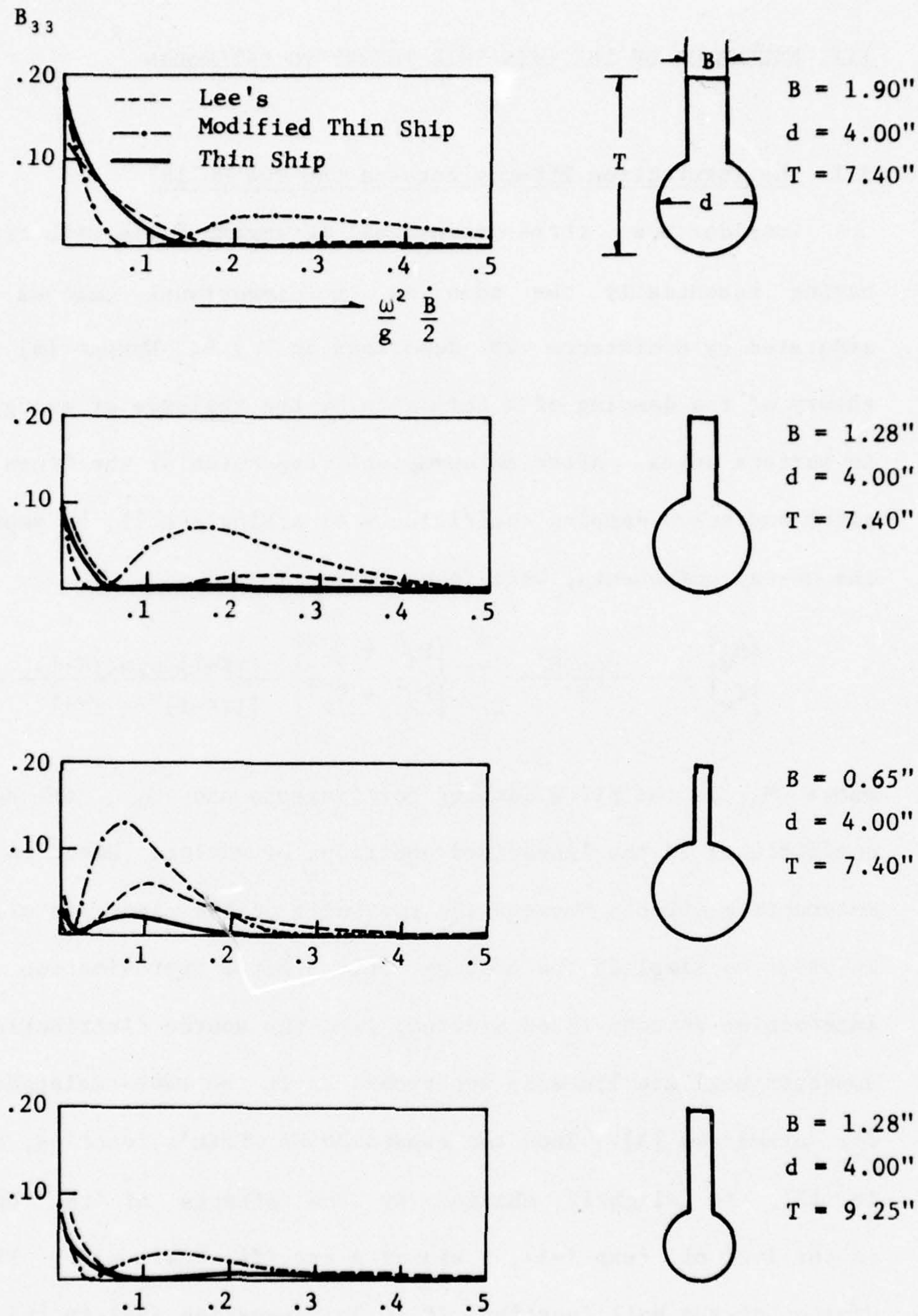

Fig. 3 Comparison of Thin-Ship and Modified Thin-Ship Results with Lee's [6]

III. EXTENSION OF THE THIN-SHIP THEORY TO CATAMARAN

3.1 The Interaction Effects Between the Two Hulls

Consider now three-dimensional catamaran hulls with cross sections having essentially the same as two-dimensional bulbous cylinders separated by a distance 2b described in Fig.4. Newman [8] developed a theory of the damping of a thin ship by the analysis of energy radiation in surface waves. After an asymptotic expansion of the Green's function, pitch and heave damping coefficients of a single hull, by separation of the energy components, were found to be:

$$\begin{Bmatrix} M_q \\ Z_w \end{Bmatrix} = - \frac{2\rho\omega\nu\beta^2}{\pi} \int_{-\infty}^{\infty} \begin{Bmatrix} P_1{}^2 + Q_1{}^2 \\ P_2{}^2 + Q_2{}^2 \end{Bmatrix} \frac{(\tau K-1)^4 \operatorname{sgn}(\tau K-1)}{[(\tau K-1)^4 - K^2]^{\frac{1}{2}}} dK \tag{3.1}$$

where M_q is the pitch damping coefficients and Z_w, the heave damping coefficients in the linearized equations of motion. Based on (3.1) the interaction effects between the two hulls of the catamaran will be included. In order to simplify the problem, only a first approximation to the hull interaction effects in considered; i.e. the source distributions of each separate hull are linearly superposed as in the wave-resistance theory for catamarans [3]. Then the expansion of Green's function, equation (66) in [8], is slightly changed by the effects of the twin hulls in the form of $\{\exp(-i\lambda_i \text{ b} \sin u) + \exp(i\lambda_i \text{ b} \sin u)\}$. Then the integration of the hull function (P_i, Q_i), equation (69) in [8], is multiplied by the same factor for catamaran hulls:

$$(P_i, Q_i)_{\text{catamaran}} = (P_i, Q_i)_{\text{single hull}} \cdot 2\cos(\lambda_i \text{ b} \sin u) \tag{3.2}$$

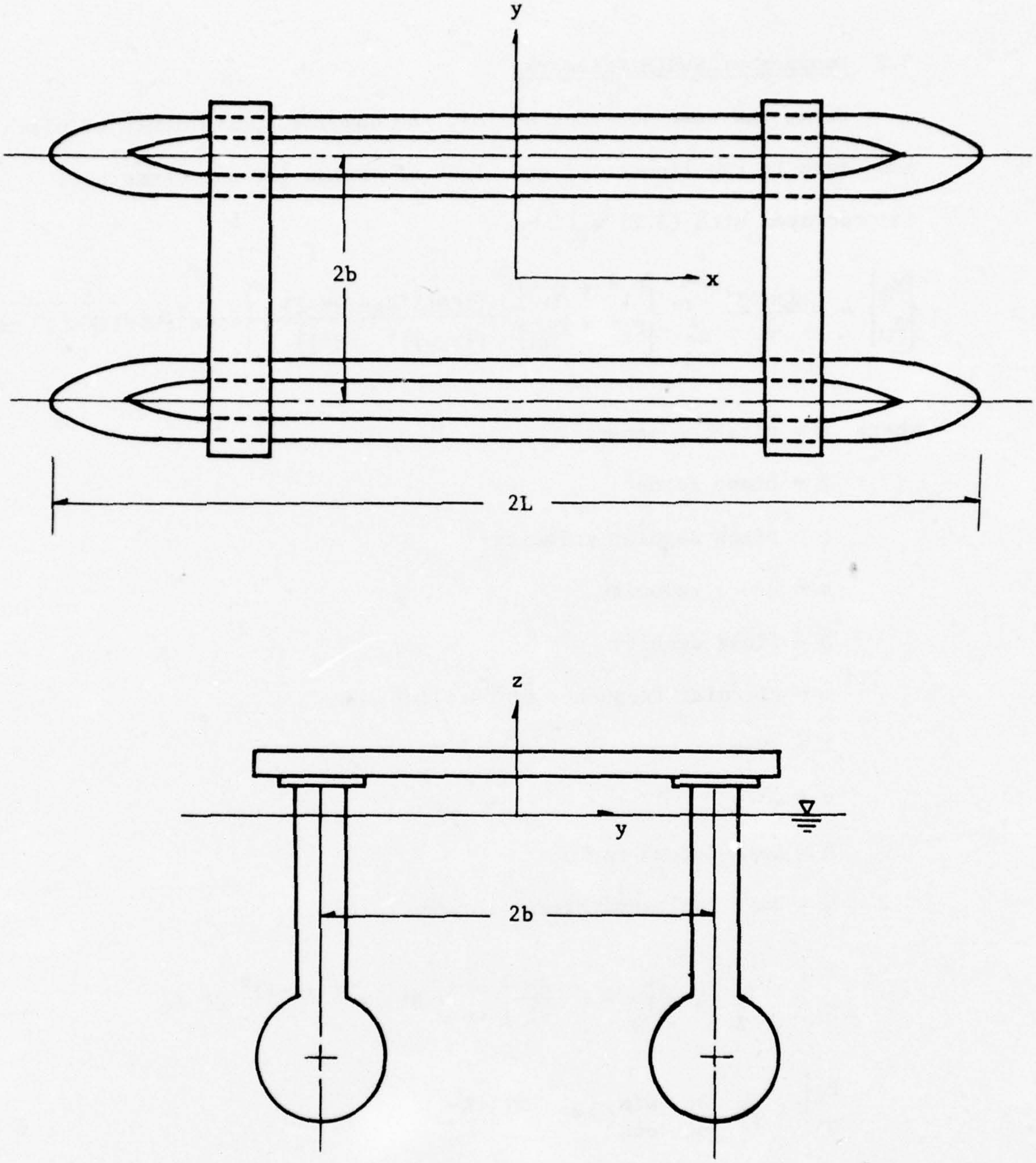

Fig. 4 Geometry of SWATH Catamaran

3.2 Damping of SWATH Catamaran

Using the same notation as [8], the damping coefficients of pitch and heave in the linearized equations of motion for catamaran hull incorporated with (3.2) will be:

$$\begin{Bmatrix} M_q \\ Z_w \end{Bmatrix} = - \frac{2\rho\omega\nu\beta^2}{\pi} \int_{-\infty}^{\infty}{}' \begin{Bmatrix} P_1{}^2 + Q_1{}^2 \\ P_2{}^2 + Q_2{}^2 \end{Bmatrix} \frac{(\tau K-1)^4 \operatorname{sgn}(\tau K-1)}{[(\tau K-1)^4 - K^2]^{\frac{1}{2}}} \left\{ 4\cos^2[\nu b\sqrt{(\tau K-1)^4 - K^2}] \right\} dK \tag{3.3}$$

where M = pitching moment

Z = heave force

q = pitch angular velocity

w = heave velocity

ρ = fluid density

ω = circular frequency of oscillations

$\tau = \omega V/g$

$\nu = \omega^2/g$

β = beam-length ratio

b = half hull separation distance

$$\begin{Bmatrix} P_1 \\ Q_1 \end{Bmatrix} = \iint_S \left(\zeta \frac{\partial h}{\partial \xi} - \xi \frac{\partial h}{\partial \zeta} \right) \frac{\sin}{\cos}(\nu K \xi)\ e^{\nu\zeta(\tau K-1)^2}\ d\xi\ d\zeta \tag{3.4}$$

$$\begin{Bmatrix} P_2 \\ Q_2 \end{Bmatrix} = \iint_S \frac{\partial h}{\partial \zeta} \frac{\sin}{\cos}(\nu K \xi)\ e^{\nu\zeta(\tau K-1)^2}\ d\xi\ d\zeta \tag{3.5}$$

The prime in equation (3.3) denotes that only the intervals of $(\tau K-1)^4 - K^2 \geq 0$ are to be included in the integration. The intervals $K_1 \leq K \leq K_2$ and $K_3 \leq K \leq K_4$ are omitted, where

$$\left.\begin{matrix} K_1 \\ \\ K_2 \end{matrix}\right\} = Re\left\{\frac{1}{2\tau^2}\left[(2\tau-1) \mp (1-4\tau)^{\frac{1}{2}}\right]\right\} \tag{3.6}$$

$$\left.\begin{matrix} K_3 \\ \\ K_4 \end{matrix}\right\} = \frac{1}{2\tau^2}\left[(2\tau+1) \mp (1+4\tau)^{\frac{1}{2}}\right] \tag{3.7}$$

Thus the integral in equation (3.3) can be decomposed in the following forms according to the values of τ :

$$\int_{-\infty}^{\infty} F(K)\, dK = \begin{cases} \displaystyle\int_{K_2}^{K_3} F(K)\, dK = I_1 & \text{if } \tau=0 \qquad (3.8) \\ \left(\displaystyle\int_{-\infty}^{K_1} + \int_{K_2}^{K_3} + \int_{K_4}^{\infty}\right) F(K)\, dK = I_2 + I_3 + I_4 & \text{if } 0<\tau<\frac{1}{4} \qquad (3.9) \\ \left(\displaystyle\int_{-\infty}^{K_3} + \int_{K_4}^{\infty}\right) F(K)\, dK = I_5 + I_6 & \text{if } \tau>\frac{1}{4} \qquad (3.10) \end{cases}$$

where $F(K)$ denotes the integrand of (3.3). Numerical procedure to evaluate the integrals in equations (3.8), (3.9) and (3.10) are described in the subsequent chapter.

3.3 The Effects of Hull Distance on Damping

It can be easily anticipated that the damping of a catamaran is affected by the hull separation distance as well as the forward speed due to the interactions between the generated waves and hulls. The equation (3.3) shows that damping is an oscillatory function of the hull distance.

For a simple case of heave damping with zero speed, the asymptotic

behavior of the damping when b is large can be readily derived. From (3.3), the heave damping integral when $\tau=0$ is:

$$Z_{\omega} = - \frac{2\rho\omega\nu\beta^2}{\pi} \int_{-1}^{1} (P_2{}^2 + Q_2{}^2) \frac{(-1)}{\sqrt{1-K^2}} 2[\cos(2\nu b\sqrt{1-K^2}) + 1]\, dK \tag{3.11}$$

In order to examine the asymptotic behavior of (3.11) for large b, consider only the oscillatory integral involving the cosine term:

$$I_1 = \int_{1}^{1} \frac{[P_2{}^2(K) + Q_2{}^2(K)]}{\sqrt{1-K^2}} \cos(2\nu b\sqrt{1-K^2})\, dK \tag{3.12}$$

From (3.5), $(P_2{}^2 + Q_2{}^2)$ can be shown to be an even function of K. Then (3.12) becomes:

$$I_1 = 2\int_{0}^{1} \frac{(P_2{}^2 + Q_2{}^2)}{\sqrt{1-K^2}} \cos(2\nu b\sqrt{1-K^2})\, dK \tag{3.13}$$

By a change of the variable, $x = \sqrt{1-K^2}$:

$$I_1 = 2\int_{0}^{1} \frac{(P_2{}^2 + Q_2{}^2)}{\sqrt{1-x^2}} \cos(2\nu bx)\, dx$$

$$= 2\int_{0}^{1} \left\{\frac{(P_2{}^2 + Q_2{}^2)}{\sqrt{1+x}}\right\} \frac{\cos(2\nu bx)}{\sqrt{1-x}}\, dx$$

$$= 2\int_{0}^{1} f(x) \frac{\cos(2\nu bx)}{\sqrt{1-x}}\, dx \tag{3.14}$$

where $f(x)$ is a regular function between $(0,1)$. By a successive integration by parts (see Copson [2]), it can be shown that the leading order asymptotic behavior as $b \to +\infty$ will be:

$$I_1 \sim \frac{1}{\sqrt{2\nu b}} \cos(2\nu b - \frac{\pi}{4}) \tag{3.15}$$

IV. NUMERICAL PROCEDURE

4.1 Zero Forward Speed Case

When $\tau=0$, K_2 and K_3 become -1 and +1 respectively. Thus equation (3.3) is reduced to the following simple form:

$$\begin{Bmatrix} M_q \\ Z_w \end{Bmatrix} = -\frac{2\rho\omega\nu\beta^2}{\pi} \int_{-1}^{+1} dK \begin{Bmatrix} P_1{}^2 + Q_1{}^2 \\ P_2{}^2 + Q_2{}^2 \end{Bmatrix} \frac{(-1)}{\sqrt{1-K^2}} \left\{4\cos^2[\nu b\sqrt{1-K^2}]\right\} \tag{4.1}$$

The integral in (4.1) is easily evaluated using the Gauss-Chebyshev quadrature formula:

$$\int_{-1}^{+1} \frac{F(K)}{\sqrt{1-K^2}} dK = \sum_{i=1}^{m} w_i \; F(K_i) + E_n \tag{4.2}$$

where K_i are the roots of the m^{th}-degree Chebyshev polynomial, so that $K_i = \cos\frac{(2i-1)\pi}{2m}$, $i=1,2,\ldots,m$; $w_i = \pi/m$; and E_n is an error term. Then (4.2) is simplified to:

$$\int_{-1}^{+1} \frac{F(K)}{\sqrt{1-K^2}} dK = \frac{\pi}{m} \sum_{i=1}^{m} F\left\{\cos\frac{2(i-1)\pi}{2m}\right\} \tag{4.3}$$

Damping coefficients are non-dimensionalized by the quantity $\rho\nabla\sqrt{g/L}$ for heave and by $\rho\nabla L\sqrt{gL}$ for pitch where ∇ is a displaced volume. Based on (4.1) and (4.3), pitch and heave damping coefficients for a single and twin hulls are calculated for the NSRDC model MODCAT. Results are plotted in Fig.6 and Fig.7.

4.2 Nonzero Forward Speed Case

If the forward speed effects are included, not only the finite integral but also the semi-infinite integrals should be evaluated. The semi-infinite integrals are quite involved due to the highly oscillatory cosine term. Consider the two cases separately according to the values of τ .

(a) $0 < \tau < 1/4$

In this case, the damping integral is decomposed in three different ranges as in (3.9). The finite integral I_3 can be treated in the same manner as the zero speed case by an appropriate change of the variable of the integration. Rewriting the finite integral:

$$I_3 = \int_{K_2}^{K_3} (P_i^{\,2} + Q_i^{\,2}) \frac{(\tau K-1)^4 \mathrm{sgn}(\tau K-1)}{\sqrt{(\tau K-1)^4 - K^2}} \cdot 4\cos^2[\nu b\sqrt{(\tau K-1)^4 - K^2}]\, dK$$

$$= \int_{K_2}^{K_3} \left\{(P_i^{\,2} + Q_i^{\,2}) \frac{(\tau K-1)^4 \mathrm{sgn}(\tau K-1)}{\tau^2\sqrt{(K_4-K)(K-K_1)}} \cdot 4\cos^2[\nu b\sqrt{(\tau K-1)^4 - K^2}]\right\} \frac{dK}{\sqrt{(K-K_2)(K_3-K)}} \tag{4.4}$$

Denoting the expression in the braces above by $F_3(K)$,

$$I_3 = \int_{K_2}^{K_3} \frac{F_3(K)}{\sqrt{(K-K_2)(K_3-K)}}\, dK \tag{4.5}$$

By a linear change of the variable of integration,

$$x = \frac{2}{K_3-K_2}(K-K_3) + 1$$

(4.5) reduces to:

$$I_3 = \int_{-1}^{1} \frac{F_3\left\{\left(\frac{K_3-K_2}{2}\right) x + \left(\frac{K_3+K_2}{2}\right)\right\}}{\sqrt{1 - x^2}}\, dx \tag{4.6}$$

where we can use Gauss-Chebyshev quadrature formula.

The semi-infinite integrals in (3.9) and (3.10) can be treated essentially in the same way. In order to facilitate the integrals, we manipulate in the following way:

$$I_2 = \int_{-\infty}^{K_1} (P_i^{\,2} + Q_i^{\,2}) \frac{(\tau K-1)^4 \operatorname{sgn}(\tau K-1)}{\sqrt{(\tau K-1)^4 - K^2}} \cdot 4\cos^2[\nu b\sqrt{(\tau K-1)^4 - K^2}]\, dK$$

$$= \int_{-\infty}^{K_1} (P_i^{\,2} + Q_i^{\,2}) \frac{(\tau K-1)^4 \operatorname{sgn}(\tau K-1)}{\tau^2\sqrt{(K_4-K)(K_3-K)(K_2-K)}} \cdot 2[\cos(2\nu b\sqrt{(\tau K-1)^4 - K^2}) + 1]\frac{dK}{\sqrt{K_1-K}}$$

$$= 2\int_{-\infty}^{K_1} \left\{(P_i^{\,2} + Q_i^{\,2}) \frac{(\tau K-1)^4 \operatorname{sgn}(\tau K-1)}{\tau^2\sqrt{(K_4-K)(K_3-K)(K_2-K)}} \cdot \cos\left[2\nu b\sqrt{(\tau K-1)^4 - K^2}\right]\right\}\frac{dK}{\sqrt{K_1-K}}$$

$$+ 2\int_{-\infty}^{K_1} (P_i^{\,2} + Q_i^{\,2}) \frac{(\tau K-1)^4 \operatorname{sgn}(\tau K-1)}{\tau^2\sqrt{(K_4-K)(K_3-K)(K_2-K)}} \frac{dK}{\sqrt{K_1-K}}$$

$$= 2(I_a + I_b) \tag{4.7}$$

where I_a denotes the first integral with an oscillatory integrand in (4.7) and I_b, the second one. Concerning only the first integral,

$$I_a = \int_{-\infty}^{K_1} \left\{(P_i^{\,2} + Q_i^{\,2}) \frac{(\tau K-1)^4 \operatorname{sgn}(\tau K-1)}{\tau^2\sqrt{(K_4-K)(K_3-K)(K_2-K)}} \cos\left[2\nu b\sqrt{(\tau K-1)^4 - K^2}\right]\right\}\frac{dK}{\sqrt{K_1-K}} \tag{4.8}$$

Dominant contributions to the integral come from the vicinity of K_1 since the oscillations get faster as $|K|$ increases, thus cancelling out effectively. Equation (4.8) can be written in the simple form:

$$I_a = \int_{-\infty}^{K_1} \frac{F_2(K)}{\sqrt{K_1-K}}\, dK \tag{4.9}$$

where $F_2(K)$ denotes the expression in the braces in (4.8). Then by a change of the variable, $x = \sqrt{K_1 - K}$:

$$I_a = 2 \int_0^{\infty} F_2(K_1 - x^2)\, dx \tag{4.10}$$

The semi-infinite integral is subdivided into an infinite number of finite ones of an interval A, so that:

$$I_a = 2 \int_0^{\infty} F_2(K_1 - x^2)\, dx = 2 \sum_{n=0}^{\infty} \int_{An}^{A(n+1)} F_2(K_1 - x^2)\, dx \tag{4.11}$$

However, due to the oscillatory nature of the integrand in (4.8), we should be very careful in choosing the size of the interval A. In order to account for the change in period of an oscillation, the interval A is chosen as the period of $\cos(2\nu b\sqrt{(\tau K-1)^4 - K^2})$. Then the sub-integrals in (4.11) are performed over these periods. As n increases, the contribution of the sub-integral gets smaller. Thus the integration can be performed to a desired accuracy by controlling the upper limit of n. After the value of A is determined, the sub-integral I_i in (4.11) for a given value of n, becomes:

$$I_i = \int_a^b F_2(K_1 - x^2)\, dx \tag{4.12}$$

where a and b are the lower and upper limits of the sub-interval. Then by a change of the variable of integration to:

$$z = \frac{2x - (a+b)}{b - a} \tag{4.13}$$

Equation (4.12) reduces to:

$$I_i = \frac{b - a}{2} \int_{-1}^{1} F_2 \left\{ K_1 - \left[\frac{z(b-a) + (a+b)}{2} \right]^2 \right\} dz \tag{4.14}$$

We now have an appropriate integral form for which we can use the Gauss-Legendre quadrature formula:

$$\int_{-1}^{1} F(z)\, dz \doteq \sum_{i=0}^{n} w_i F(z_i) \tag{4.15}$$

where w_i are weight factors given by:

$$w_i = \int_{-1}^{1} \prod_{\substack{j=0 \\ j\neq i}}^{n} \left[\frac{z - z_j}{z_i - z_j} \right] dz \tag{4.16}$$

and z_i are the roots of the Legendre Polynomial $P_{n+1}(z)$. The roots z_i and the weight factors w_i for several values of n are listed in Table 1.

For the integral I_4 , the same procedure can be used as in I_2 except for a different change of the variable of the integration. From (3.9),

$$I_4 = \int_{K_4}^{\infty} F_4(K) \frac{dK}{\sqrt{K-K_4}} \tag{4.17}$$

where

$$F_4(K) = (P_i^{\,2} + Q_i^{\,2}) \left\{ \frac{(\tau K-1)^4 \operatorname{sgn}(\tau K-1)}{\tau^2 \sqrt{(K-K_1)(K-K_2)(K-K_3)}} \right\} \left\{ 4\cos^2 \left[\nu b \sqrt{(\tau K-1)^4 - K^2} \right] \right\}$$

By changing of the variable, $x = \sqrt{K - K_4}$:

$$I_4 = 2 \int_{0}^{\infty} F_4(K_4+x^2)\, dx \tag{4.18}$$

Analogous to (4.11), we subdivide the semi-infinite integral into finite ones:

$$I_4 = 2 \sum_{n=0}^{\infty} \int_{An}^{A(n+1)} F_4(K_4+x^2)\, dx \tag{4.19}$$

By the same change of the variable (4.13), each sub-integral in (4.19) reduces to:

$$I_i = \frac{b-a}{2} \int_{-1}^{1} F_4 \left\{ K_4 + \left[\frac{z(b-a) + (a+b)}{2} \right]^2 \right\} dz \qquad (4.20)$$

where the Gauss-Legendre quadrature formula (4.15) and (4.16) may be used.

(b) $\underline{\tau > 1/4}$

When $\tau > 1/4$, we have two integrals I_5 and I_6 similar to I_2 and I_4 . Briefly repeating the same procedure as in I_2 and I_4 :

$$I_5 \quad \int_{-\infty}^{K_3} F_5(K) \frac{dK}{\sqrt{K_3 - K}} \qquad (4.21)$$

and

$$I_6 = \int_{K_4}^{\infty} F_6(K) \frac{dK}{\sqrt{K - K_4}} \qquad (4.22)$$

where

$$F_5(K) = (P_i^{\ 2} + Q_i^{\ 2}) \left\{ \frac{(\tau K-1)^4 \mathrm{sgn}(\tau K-1)}{\tau\sqrt{[(\tau K-1)^2 + K](K_4 - K)}} \right\} \left\{ 4\cos^2\left[\nu b\sqrt{(\tau K-1)^4 - K^2} \right] \right\} \qquad (4.23)$$

and

$$F_6(K) = (P_i^{\ 2} + Q_i^{\ 2}) \left\{ \frac{(\tau K-1)^4 \mathrm{sgn}(\tau K-1)}{\tau\sqrt{[(\tau K-1)^2 + K](K - K_3)}} \right\} \left\{ 4\cos^2\left[\nu b\sqrt{(\tau K-1)^4 - K^2} \right] \right\} \qquad (4.24)$$

By changing the variables, $x = \sqrt{K_3 - K}$ for (4.21) and $x = \sqrt{K - K_4}$ for (4.22), (4.21) and (4.22) reduce to:

$$I_5 = 2 \int_0^{\infty} F_5(K_3 - x^2)\, dx \qquad (4.25)$$

and

$$I_6 = 2 \int_0^{\infty} F_6(K_4 - x^2)\, dx \qquad (4.26$$

where we can use the Gauss-Legendre quadrature formula for each sub-integral after dividing the semi-infinite integrals into finite ones as done for I_2 and I_4 .

$$\int_{-1}^{1} F(z)\,dz = \sum_{i=0}^{n} w_i F(z_i)$$

Roots (z_i)	Weight Factors (w_i)
Two-Point Formula $n = 1$	
$\pm 0.57735\ 02691\ 89626$	1.00000 00000 00000
Three-Point Formula $n = 2$	
0.00000 00000 00000	0.88888 88888 88889
$\pm 0.77459\ 66692\ 41483$	0.55555 55555 55556
Four-Point Formula $n = 3$	
$\pm 0.33998\ 10435\ 84856$	0.65214 51548 62546
$\pm 0.86113\ 63115\ 94053$	0.34785 48451 37454
Five-point Formula $n = 4$	
0.00000 00000 00000	0.56888 88888 88889
$\pm 0.53846\ 93101\ 05683$	0.47862 86704 99366
$\pm 0.90617\ 98459\ 38664$	0.23692 68850 56189
Six-Point Formula $n = 5$	
$\pm 0.23861\ 91860\ 83197$	0.46791 39345 72691
$\pm 0.66120\ 93864\ 66265$	0.36076 15730 48139
$\pm 0.93246\ 95142\ 03152$	0.17132 44923 79170
Ten-Point Formula $n = 9$	
$\pm 0.14887\ 43389\ 81631$	0.29552 42247 14753
$\pm 0.43339\ 53941\ 29247$	0.26926 67193 09996
$\pm 0.67940\ 95682\ 99024$	0.21908 63625 15982
$\pm 0.86506\ 33666\ 88985$	0.14945 13491 50581
$\pm 0.97390\ 65285\ 17172$	0.06667 13443 08688
Fifteen-Point Formula $n = 14$	
0.00000 00000 00000	0.20257 82419 25561
$\pm 0.20119\ 40939\ 97435$	0.19843 14853 27111
$\pm 0.39415\ 13470\ 77563$	0.18616 10001 15562
$\pm 0.57097\ 21726\ 08539$	0.16626 92058 16994
$\pm 0.72441\ 77313\ 60170$	0.13957 06779 26154
$\pm 0.84820\ 65834\ 10427$	0.10715 92204 67172
$\pm 0.93727\ 33924\ 00706$	0.07036 60474 88108
$\pm 0.98799\ 25180\ 20485$	0.03075 32419 96117

Table 1. Roots of the Legendre Polynomials $P_{n+1}(z)$ and the Weight Factors for the Gauss-Legendre Quadrature [1]

4.3 The Integration of the Hull Function (P_i, Q_i)

In section 3.2, (P_i, Q_i) were defined as:

$$\begin{Bmatrix} P_1 \\ Q_1 \end{Bmatrix} = \int_{-L}^{L} \left\{ \int_{-T}^{0} \left(\zeta \frac{\partial h}{\partial \xi} - \xi \frac{\partial h}{\partial \zeta} \right) e^{\nu\zeta(\tau K-1)^2} d\zeta \right\} \begin{matrix} \sin \\ \cos \end{matrix} (\nu K \xi)\, d\xi \qquad (4.27)$$

and

$$\begin{Bmatrix} P_2 \\ Q_2 \end{Bmatrix} = \int_{-L}^{L} \left\{ \int_{-T}^{0} \frac{\partial h}{\partial \zeta} e^{K\zeta(\tau K-1)^2} d\zeta \right\} \begin{matrix} \sin \\ \cos \end{matrix} (\nu K \xi)\, d\xi \qquad (4.28)$$

where $i = 1$ is for pitch and $i = 2$, for heave. Since the integrals in the braces are functions of K, τ and ξ, they can be easily evaluated numerically for given values of K, τ and for a given section. After the sectional integration, integrations along the length of the hull are performed. If the values of ν, τ and K are given and if we let the inner integrals in (4.27) and (4.28) be $f_i(\xi)$, then:

$$\begin{Bmatrix} P_i \\ Q_i \end{Bmatrix} = \int_{-L}^{L} f_i(\xi) \begin{Bmatrix} \sin\alpha\xi \\ \cos\alpha\xi \end{Bmatrix} d\xi \qquad \begin{matrix} i = 1;\ \text{pitch} \\ i = 2;\ \text{heave} \end{matrix} \qquad (4.29)$$

where α is some constant. The integral of the form (4.29) can be evaluated using the concept of the Filon-Trapezoidal quadrature [12]. The basic idea is to approximate $f_i(\xi)$ by a linear function $(a_i\xi + b_i)$, say, between the intervals ξ_i and ξ_{i+1}. Then (P_i, Q_i) can be approximated:

$$\begin{Bmatrix} P_i \\ Q_i \end{Bmatrix} \doteq \sum_{i=1}^{N} \int_{\xi_i}^{\xi_{i+1}} (a_i\xi + b) \begin{Bmatrix} \sin\alpha\xi \\ \cos\alpha\xi \end{Bmatrix} d\xi \qquad (4.30)$$

where $\xi_1 = -L$ and $\xi_{N+1} = L$.

V. RESULTS AND DISCUSSIONS

A computer program in Fortran IV, based on the analysis of this report, has been developed, and calculations have been performed for the sample model (Fig. 5) for several Froude numbers using the IBM 360/370 computer at the MIT Information Processing Center.

As input data, we must supply the offsets of each section of the hull. If there is a parallel middle body, we need to give only the offsets of the beginning and ending sections of the parallel middle body. The offsets of the remaining sections in the parallel middle body can be omitted. For instance, the offsets of the stations 9 and 11 are sufficient to take care of the parallel middle body in the sample model (Fig. 5).

The most time-consuming computer operations occur when evaluating the semi-infinite integrals, especially due to the highly oscillatory cosine term for twin hulls. Numerical convergence of these integrals becomes slower as the Froude number increases.

Calculations were made for Froude numbers 0.0, 0.2, and 0.4. In Figures 6 through 11, theoretical heave damping coefficients are compared with Lee's experiments [6]. In Tables 3 through 5, computer outputs of theoretical pitch damping coefficients are listed. It is to be noted in particular that the pitch damping coefficient for Froude number 0.4 at low frequencies becomes negative (Table 5). The negative damping in the present study is not easy to explain. But if it is physically realistic, it implies that the ship will be unstable in pitch at high speed. The presence of negative damping was noticed for an oscillating ellipsoid

near a free surface by Newman [9] and by Gerritsma, Kerwin and Newman [5] for the Series 60 hull forms. In the present case, where the hull geometry is such that zero or minimal damping can occur at zero speed, one anticipates that negative damping may occur sooner than was observed in [5] and [9].

In both Figures and Tables, it is to be noted that when the forward speed effects are considered there are peak values of damping coefficients at critical frequencies; 1.25 at $F_n = 0.2$ and 0.625 at $F_n = 0.4$ for which $\tau = 1/4$. Although the qualitative agreement is good, the theoretical predictions are seen to be somewhat lower in the higher frequency range and higher in the lower frequency range, especially near the critical frequencies at $\tau = 1/4$.

In Figures 2 and 3, thin-ship and modified thin-ship results for two-dimensional cylindrical bodies are compared with Frank's [4] and Lee's [6] works. Correction factors in the modified thin-ship approach may vary depending on the hull forms and the frequencies. At high frequencies the modified thin-ship results with a correction factor of 2 give excessive damping, but in the frequency range of practical importance this modified theory agrees better with Frank's and Lee's results than does the pure thin-ship theory.

In Figures 12 through 14, damping coefficients are plotted against hull distance variations for Froude numbers 0.0, 0.05 and 0.4 at a fixed non-dimensionalized frequency 4.0. In order to investigate the Brard parameter influence on damping as well, Froude numbers are chosen such that $\tau = 0.0$, 0.2 and 1.6 for each case. In Figure 12 it is verified that heave damping coefficients at zero forward speed oscillate

with a period of $\lambda/2$ and the mean amplitude of oscillations decays almost like $(2\nu b)^{-1/2}$, which was derived in (3.5) by the asymptotic analysis. As the hull distance and Brard parameter increase, the oscillatory phenomenon dies out faster. The diminished interference effects at higher Brard numbers can be explained physically by the fact that the waves in this case are confined to progressively smaller angles downstream. Hence the waves will not impinge upon the opposite hulls if the Brard number is sufficiently large. The minimum hull separation distance at which the interaction effects cease can be predicted by finding the generated wave angles from Fig. 1 in [8].

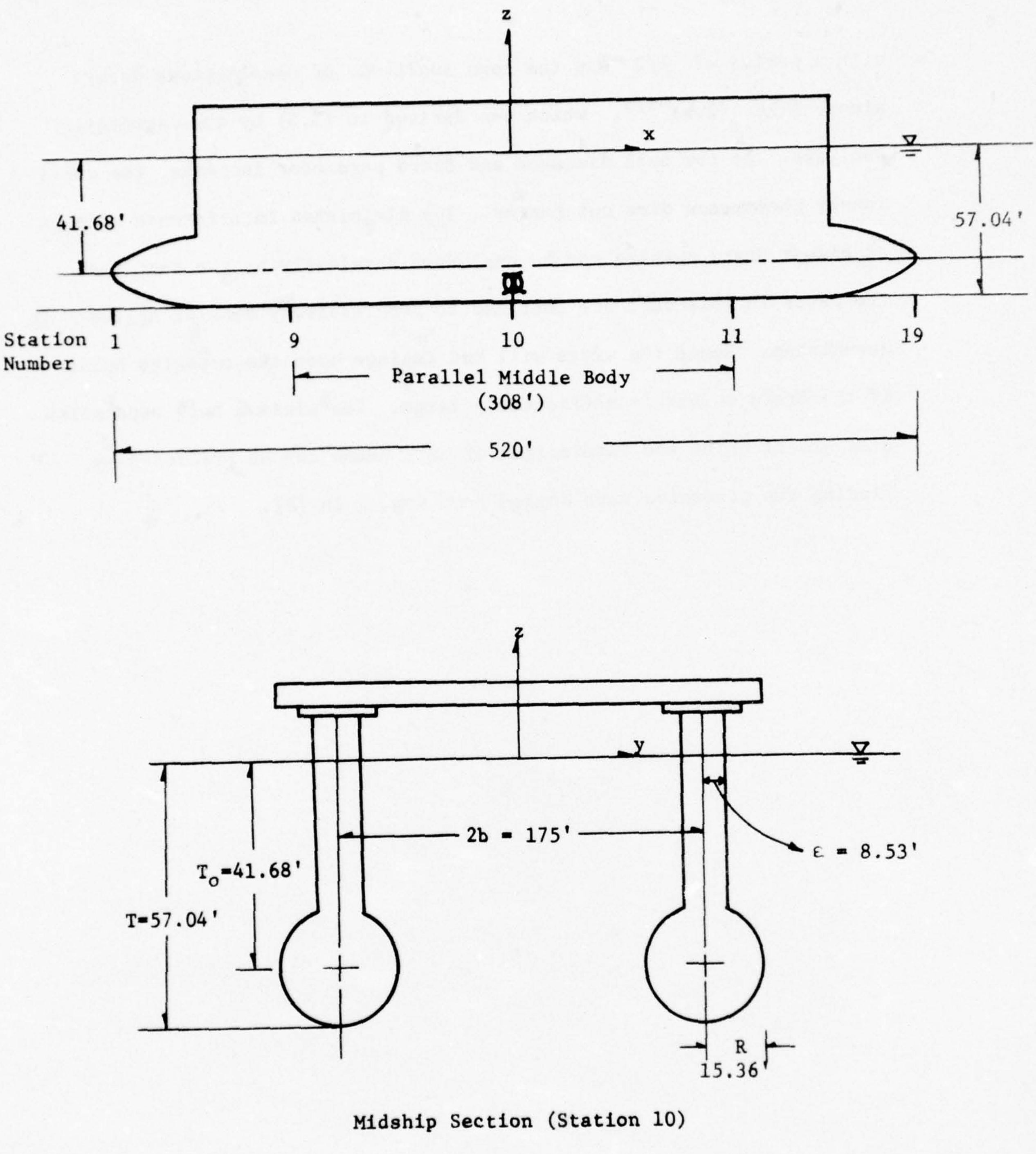

Fig. 5 Dimensions of SWATH Catamaran for the Sample Program

STN	X(I)	EPS(I)	TO(I)	R(I)
1	-261.00	0.00	41.68	0.00
2	-250.00	0.00	41.68	5.46
3	-240.60	0.00	41.68	11.16
4	-230.00	0.00	41.68	13.38
5	-220.00	1.52	41.68	14.27
6	-209.00	3.04	41.68	15.19
7	-198.00	5.19	41.68	15.36
8	-176.00	7.85	41.68	15.36
9	-154.00	8.53	41.68	15.36
10	0.00	8.53	41.68	15.36
11	154.00	8.53	41.68	15.36
12	176.00	9.72	41.68	15.29
13	198.00	5.12	41.68	14.37
14	209.00	2.87	41.68	13.48
15	220.00	1.44	41.68	12.32
16	229.80	0.00	41.68	10.62
17	239.50	0.00	41.68	8.09
18	249.50	0.00	41.68	4.61
19	259.00	0.00	41.68	0.00

Table 2. Offset Data for the Sample Program

Froude Number = 0.0

B_{55} = Pitch Damping Coefficient

$$= \frac{\text{Damping}}{\rho \nabla L \sqrt{gL}}$$

∇ = Displaced Volume

ω_e = Encountering Frequency = ω at F_n=0.0

$\omega_e\sqrt{L/g}$	B_{55} Single Hull	B_{55} Twin Hulls
0.5	0.10851E-05	0.21689E-05
1.0	0.64874E-04	0.12846E-03
1.5	0.17057E-03	0.32428E-03
2.0	0.10922E-03	0.14321E-03
2.5	0.25516E-02	0.15228E-02
3.0	0.96172E-02	0.37951E-02
3.5	0.17570E-01	0.13984E-01
4.0	0.20316E-01	0.35164E-01
4.5	0.18057E-01	0.19299E-01
5.0	0.14401E-01	0.33401E-02
5.5	0.95581E-02	0.14782E-01
6.0	0.54997E-02	0.56590E-02
6.5	0.28302E-02	0.13068E-02

Table 3. Theoretical Results of the Pitch Damping Coefficients

Froude Number = 0.2

B_{55} = Pitch Damping Coefficient

$$= \frac{\text{Damping}}{\rho \nabla L \sqrt{gL}}$$

∇ = Displaced Volume

ω_e = Encountering Frequency

$\omega_e \sqrt{L/g}$	B_{55} Single Hull	B_{55} Twin Hulls
1.00	0.78276E-02	0.39147E-02
1.25	0.18242E-01	0.23052E-01
1.50	0.91238E-02	0.58606E-02
2.00	0.80448E-02	0.57695E-02
2.50	0.93458E-02	0.70857E-02
3.00	0.10716E-01	0.13841E-01
3.50	0.11544E-01	0.14518E-01
4.00	0.11595E-01	0.71407E-02
4.50	0.10893E-01	0.12743E-01
5.00	0.97016E-02	0.13490E-01

Table 4. Theoretical Results of the Pitch Damping Coefficients

Froude Number = 0.4

B_{55} = Pitch Damping Coefficient

$$= \frac{\text{Damping}}{\rho \nabla L \sqrt{gL}}$$

∇ = Displaced Volume

ω_e = Encountering Frequency

$\omega_e \sqrt{L/g}$	B_{55} Single Hull	B_{55} Twin Hulls
0.250	-0.81562E-02	0.66851E-03
0.500	-0.64218E-02	-0.30374E-02
0.625	-0.12086E-02	0.29785E-02
0.750	-0.24313E-02	-0.38668E-02
1.000	0.20595E-02	-0.21786E-02
1.500	0.78046E-02	0.51413E-02
2.000	0.84687E-02	0.10173E-01
2.500	0.88749E-02	0.11627E-01
3.000	0.88978E-02	0.95881E-02
3.500	0.73347E-02	0.60902E-02
4.000	0.58270E-02	0.46028E-02
4.500	0.54560E-02	0.54672E-02
5.000	0.54788E-02	0.63667E-02
5.500	0.52273E-02	0.60154E-02
6.000	0.47029E-02	0.49008E-02
6.500	0.39953E-02	0.37948E-02
7.000	0.31860E-02	0.29722E-02
7.500	0.24167E-02	0.23651E-02

Table 5. Theoretical Results of the Pitch Damping Coefficients

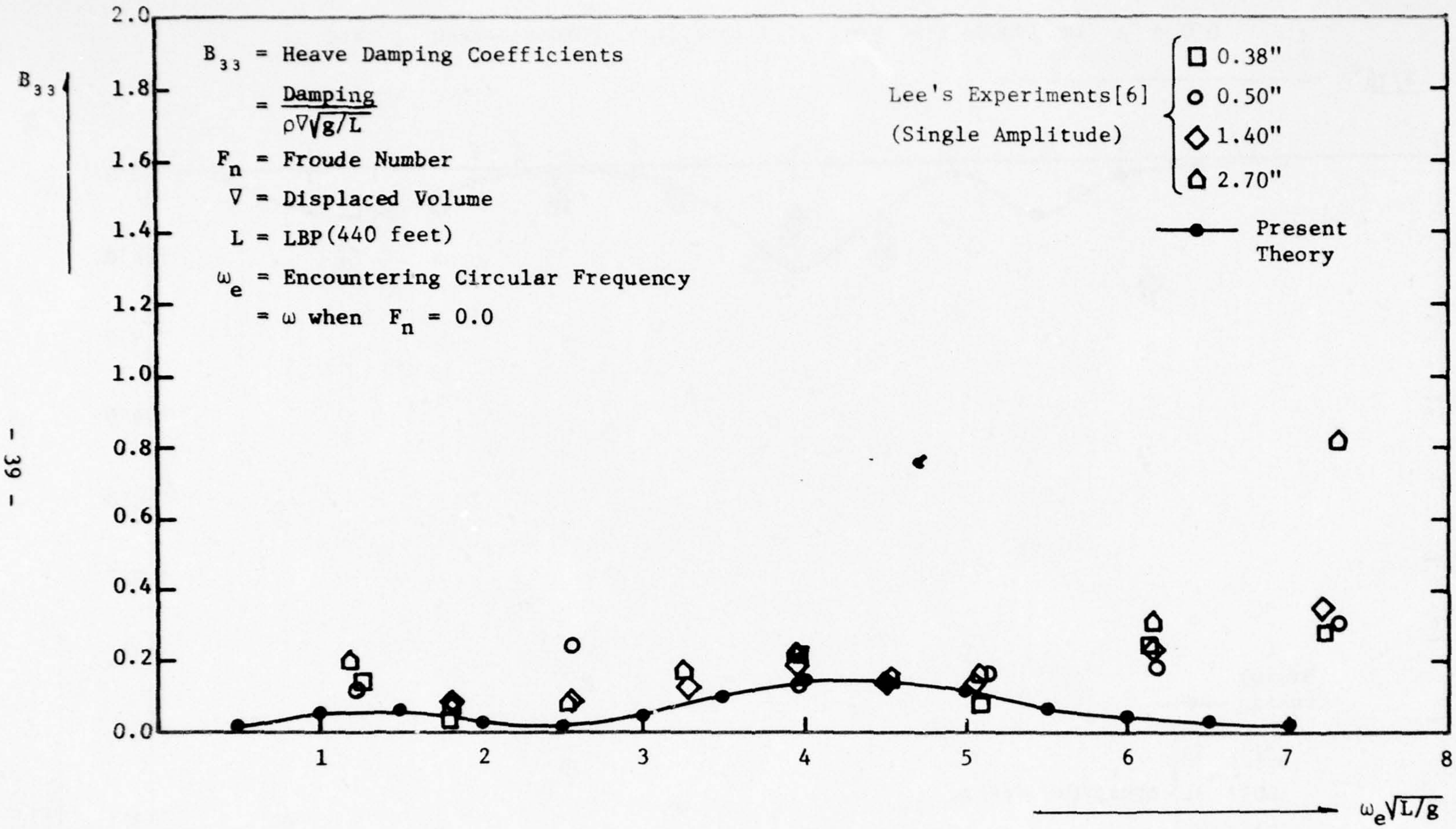

Fig. 6 Heave Damping Coefficients of Single Hull MODCAT at F_n = 0.0

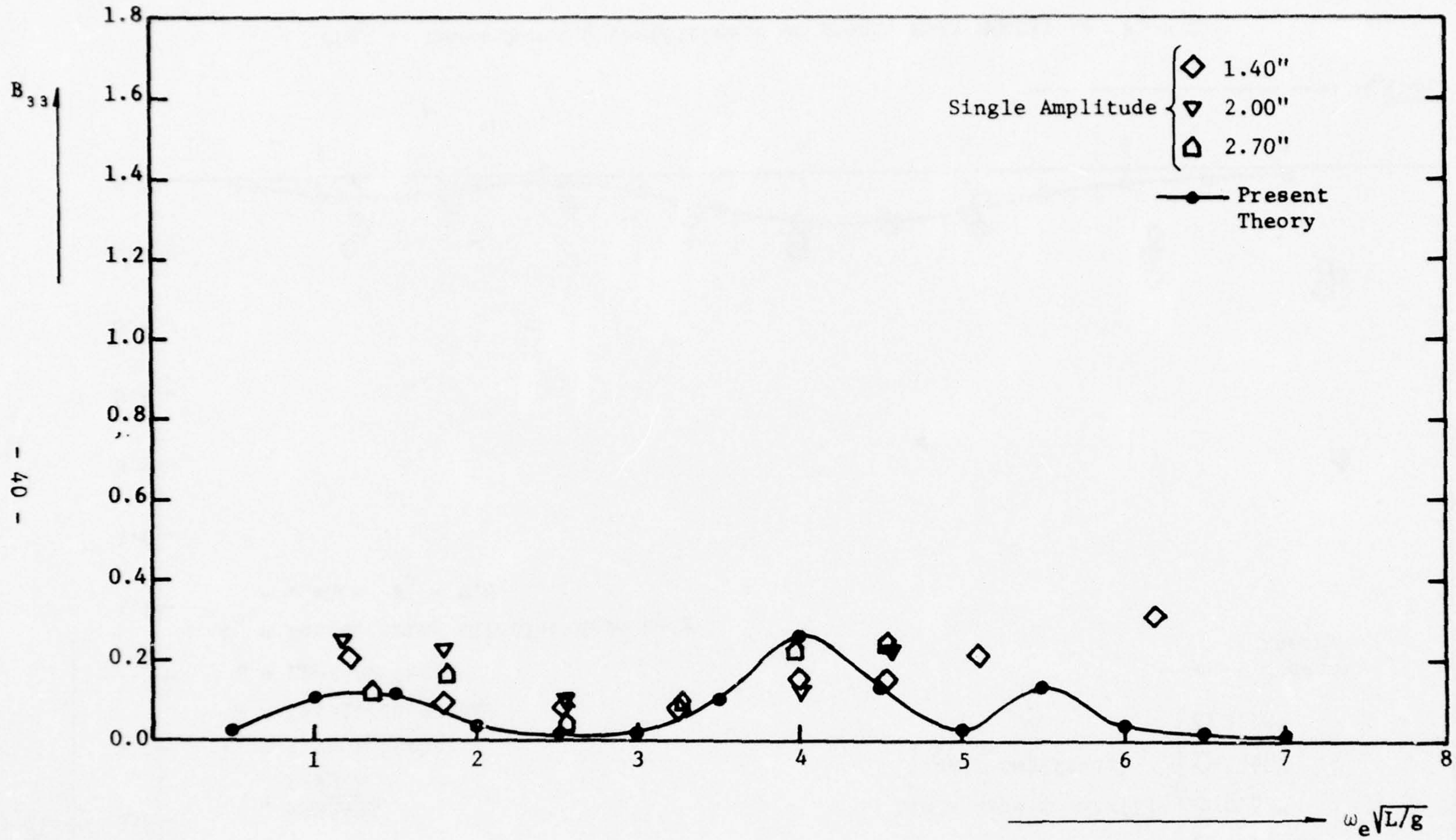

Fig. 7 Heave Damping Coefficients of Twin Hull MODCAT at $F_n = 0.0$

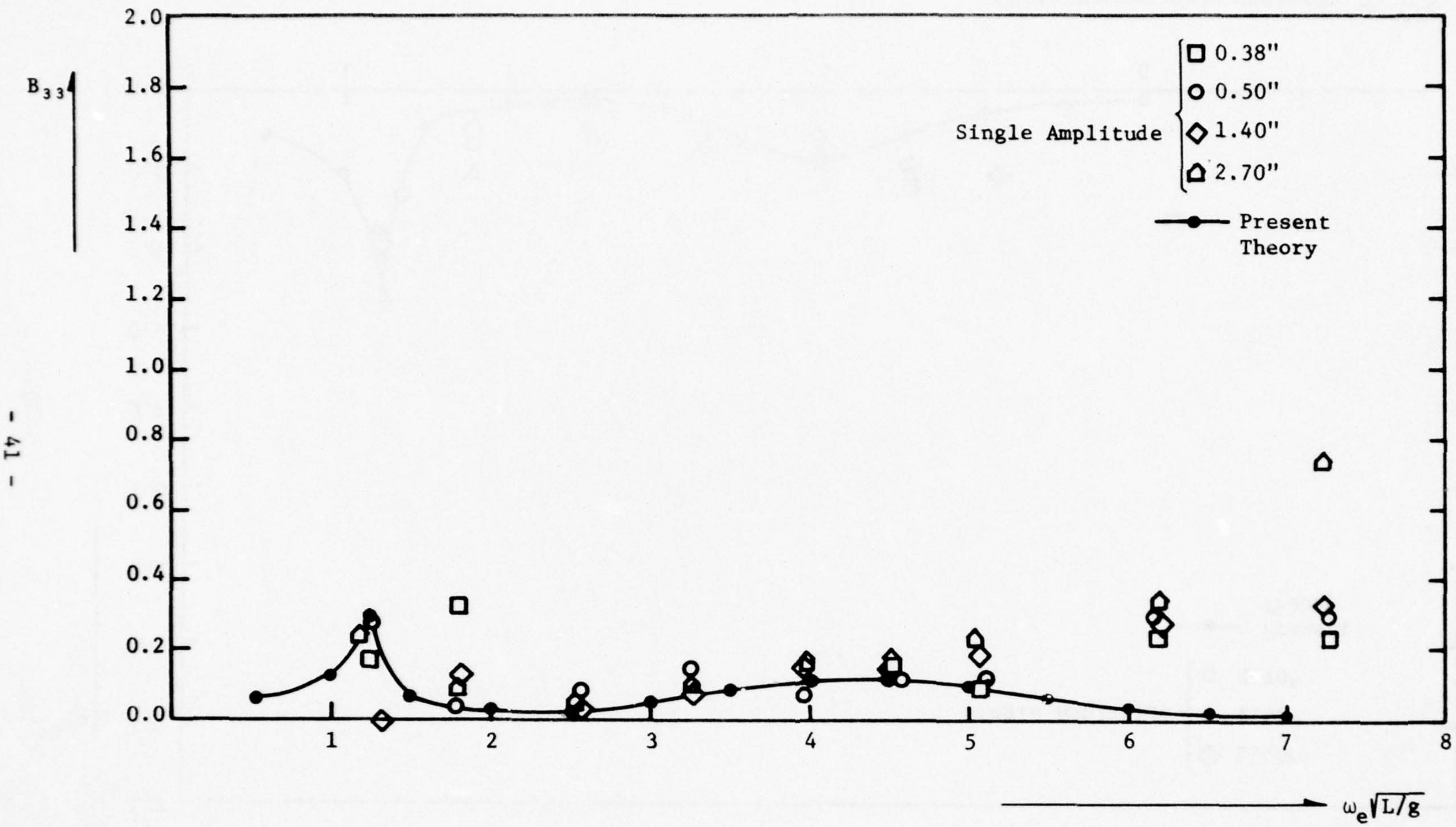

Fig. 8 Heave Damping Coefficients of Single Hull MODCAT at F_n = 0.20

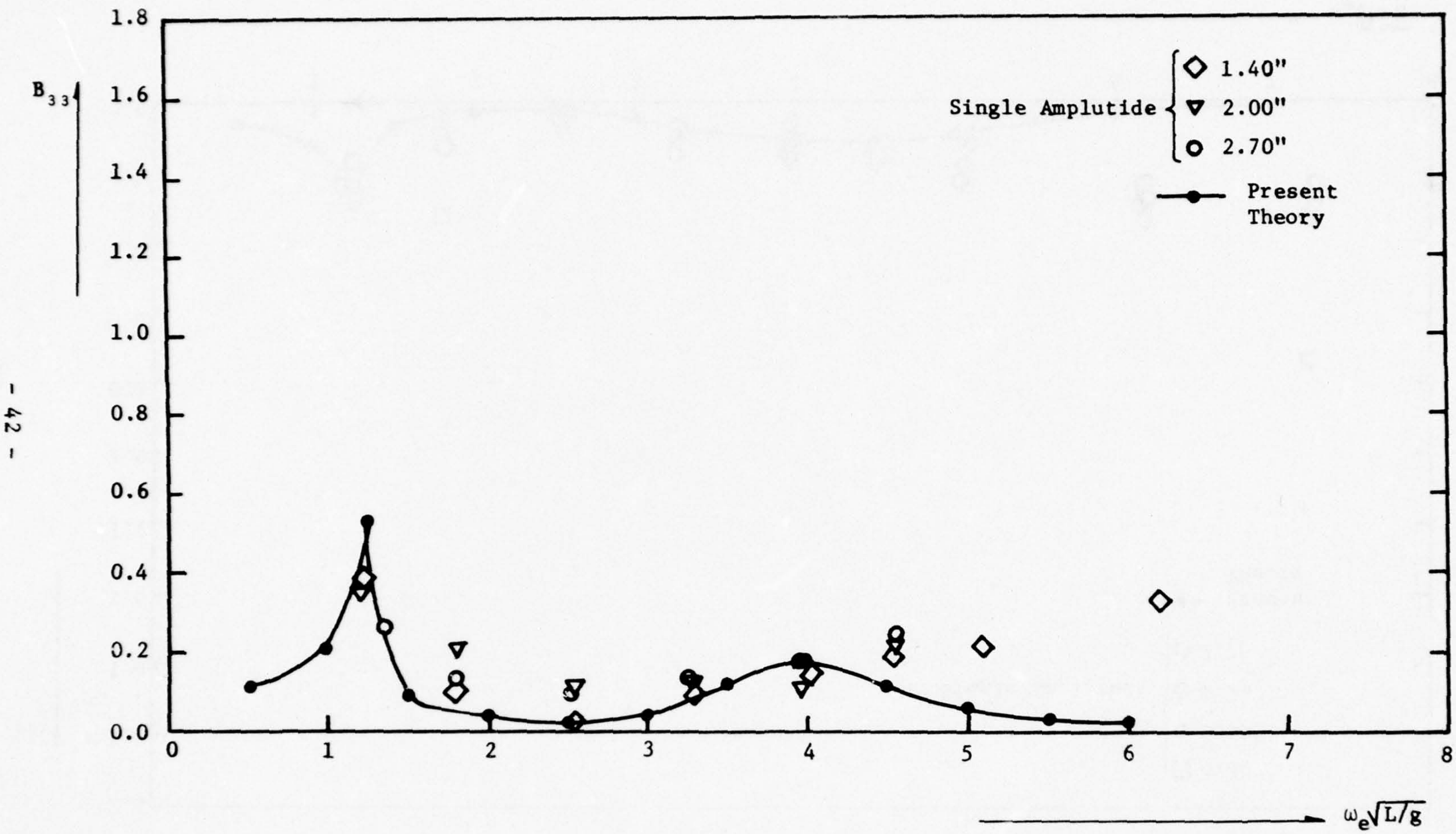

Fig. 9 Heave Damping Coefficients of Twin Hull MODCAT at $F_n = 0.20$

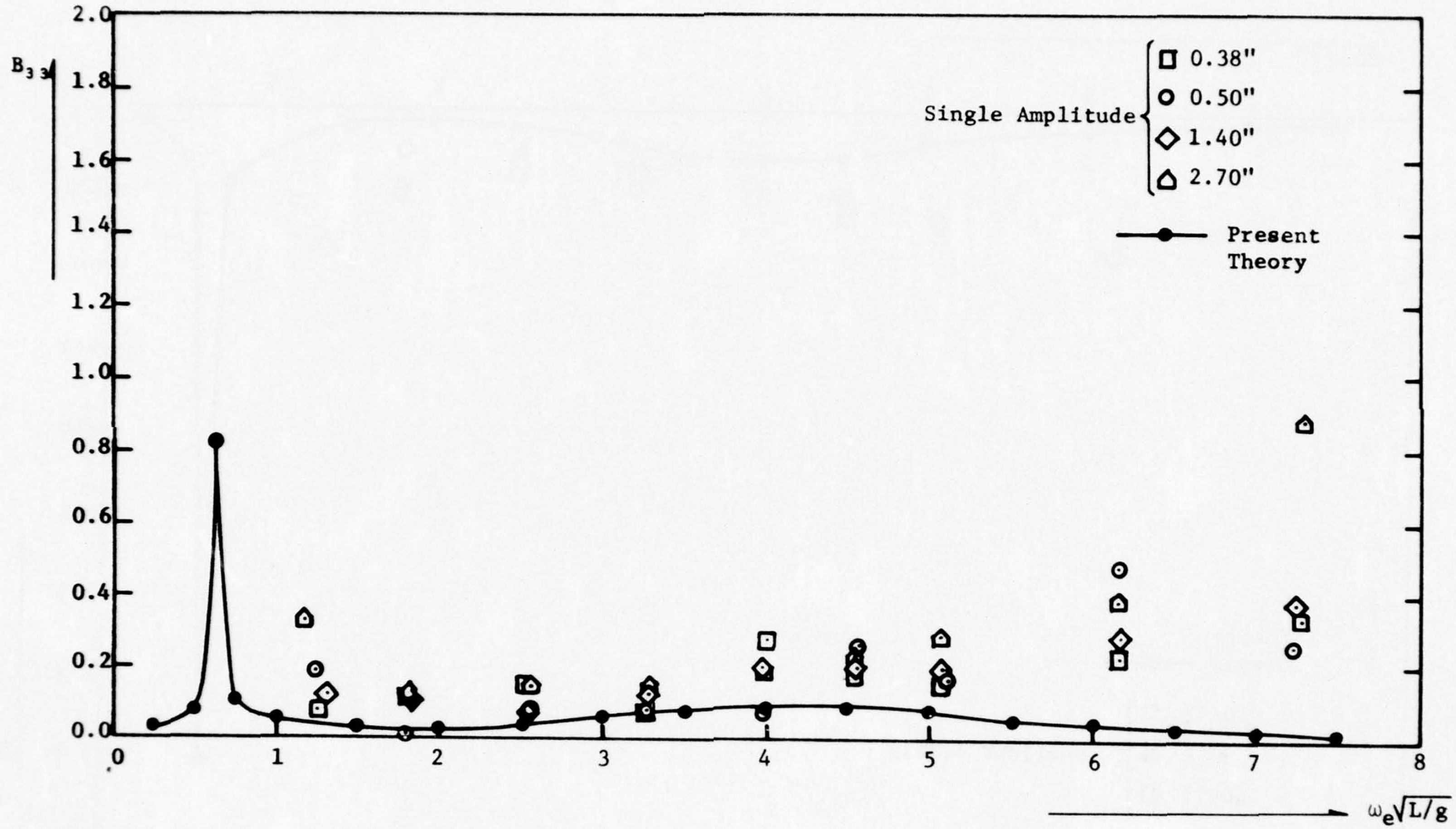

Fig. 10 Heave Damping Coefficients of Single Hull MODCAT at $F_n = 0.40$.

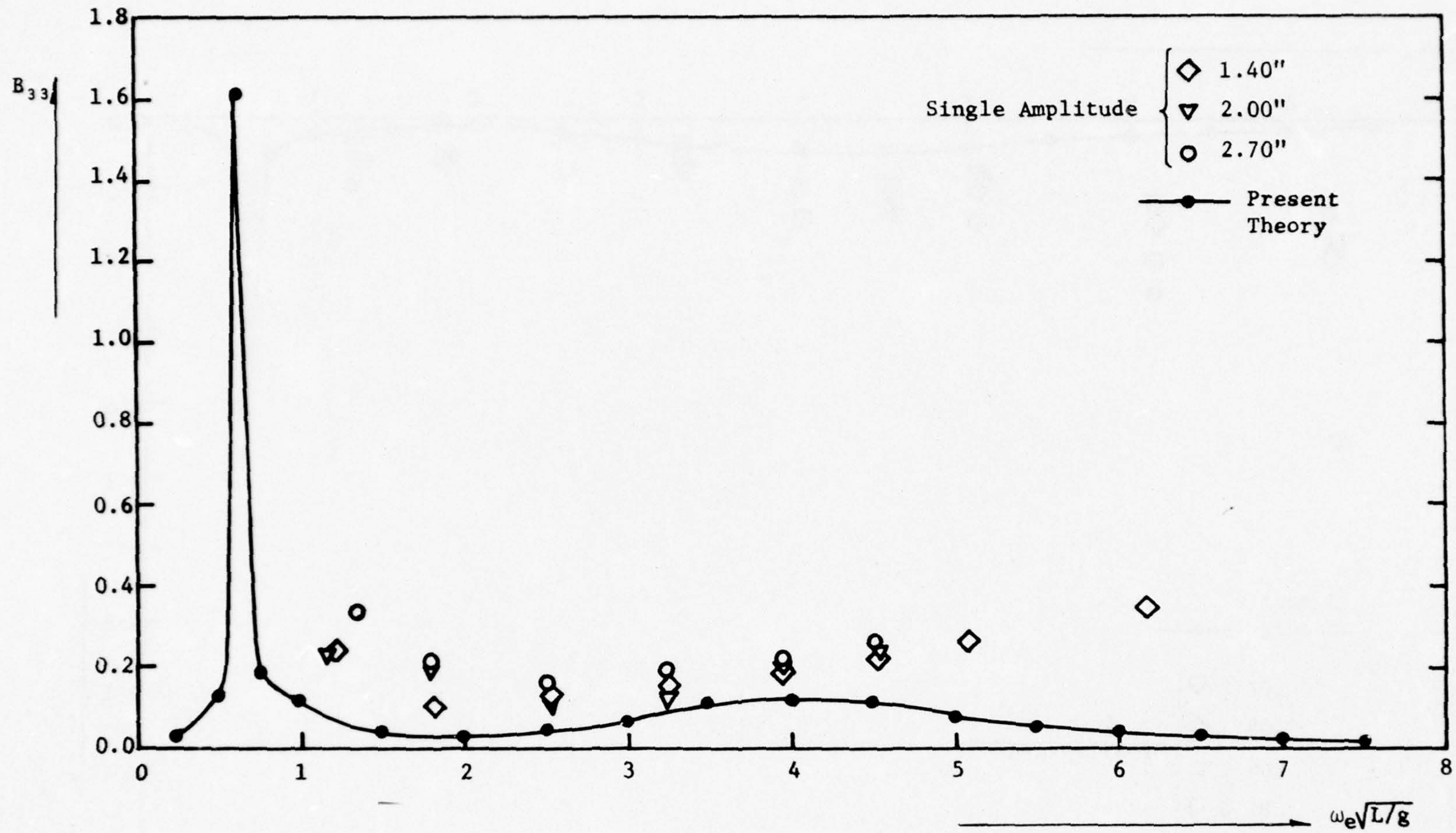

Fig. 11 Heave Damping Coefficients of Twin Hull MODCAT at $F_n = 0.40$

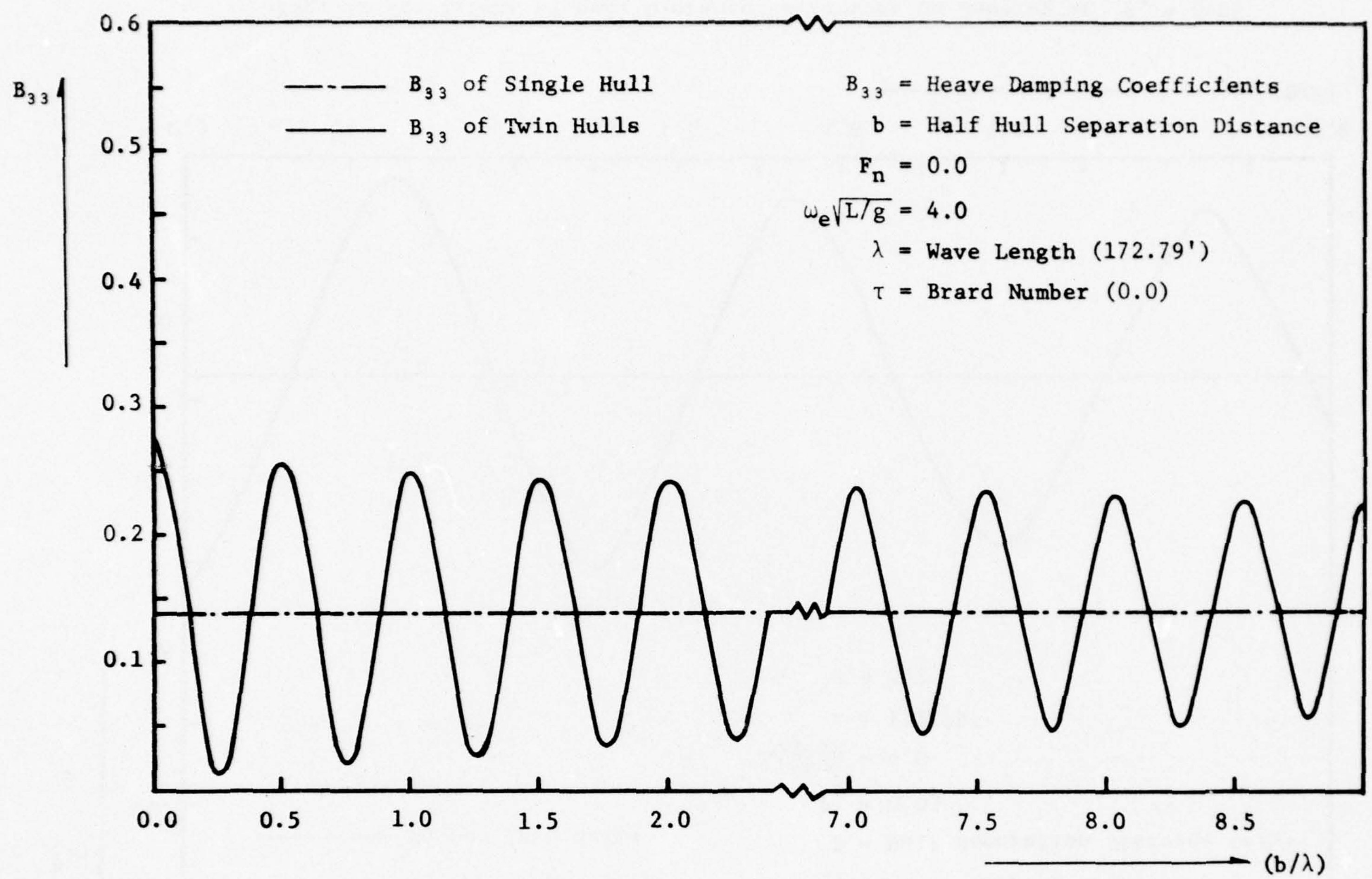

Fig. 12 The Effect of Hull Distance Vairations on Damping at $F_n = 0.0$

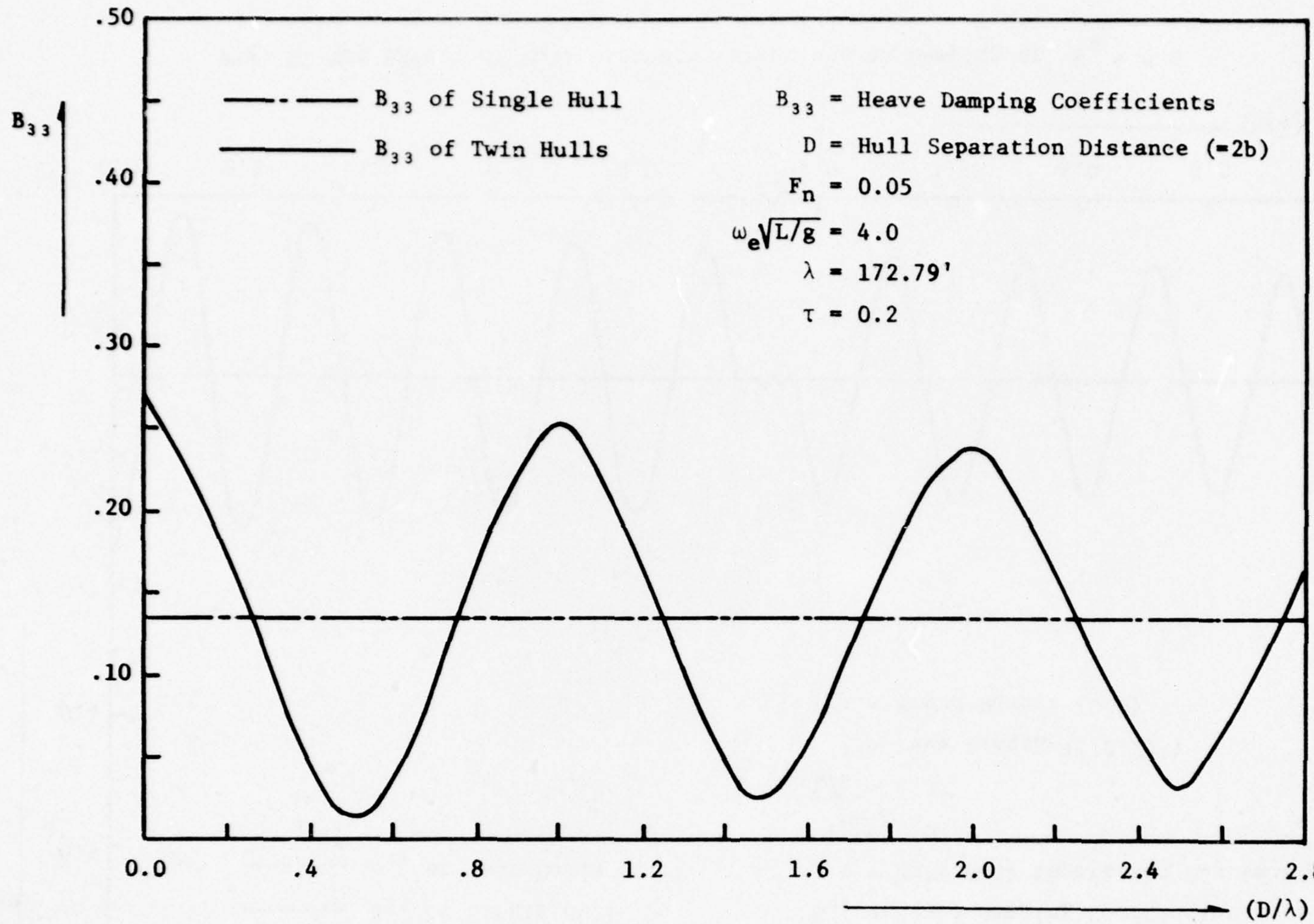

Fig. 13 The Effect of Hull Distance Variations on Damping at $F_n = 0.05$

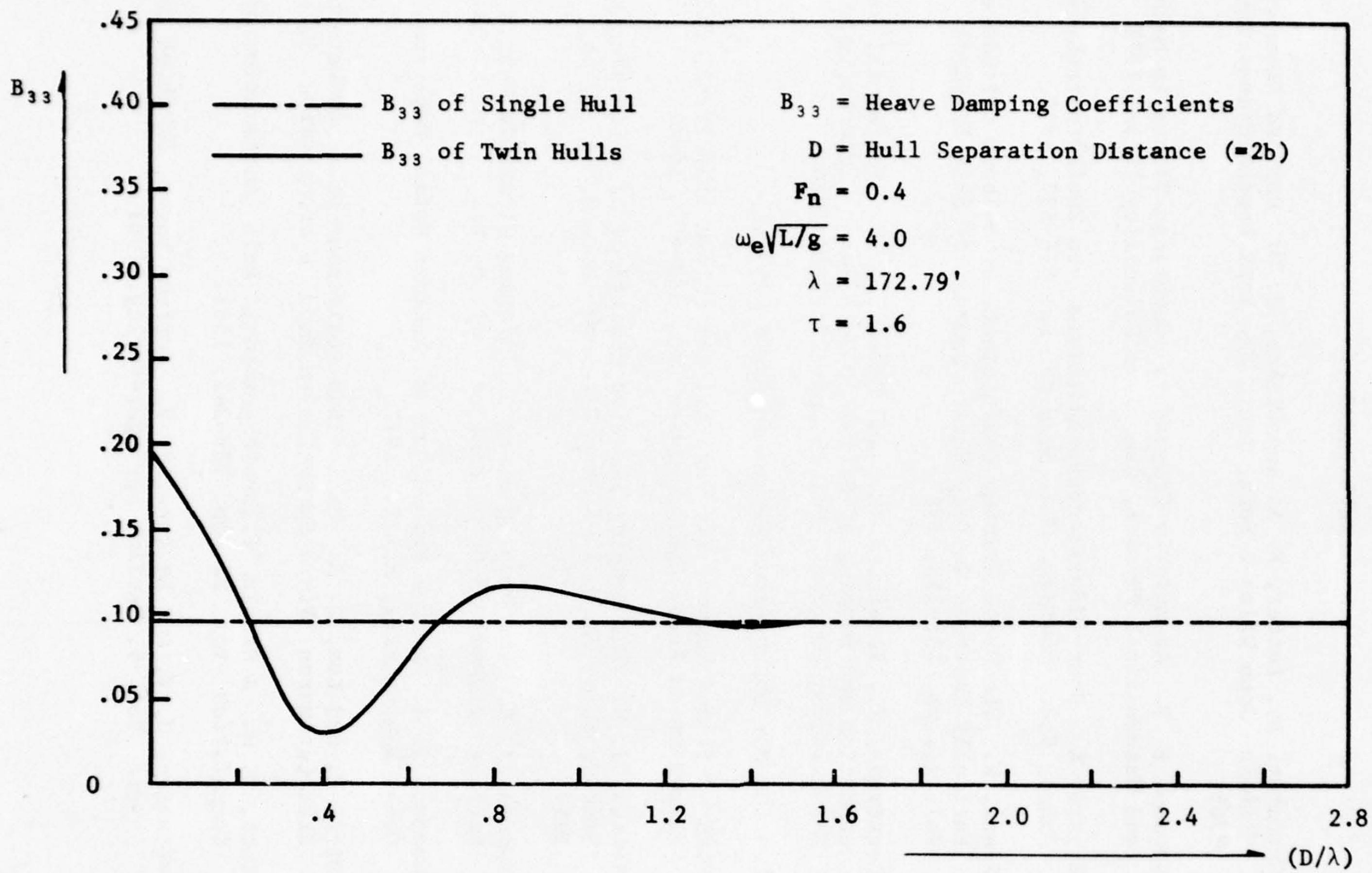

Fig. 14 The Effect of Hull Distance Variations on Damping at $F_n = 0.4$

REFERENCES

1. Carnahan, B., Luther, H. A. and Wilkes, J. O. *Applied Numerical Methods* John Wiley & Sons, Inc., New York.London.Sydney.Toronto, 1969.

2. Copson, E. T. *Asymptotic Expansions* Cambridge Tracts in Mathematics and Mathematical Physics, Cambridge University Press, 1971.

3. Eggers, K. Über Widerstandsverhaltnisse von Zweikörperschiffen *Jahrb. Schiffbautech. Ges. Band 49* pp. 516-537, 1955.

4. Frank, W. The Heave Damping Coefficients of Bulbous Cylinders, Partially Immersed in Deep Water *Journal of Ship Research* Vol. 11, pp. 151-153, 1967.

5. Gerritsma, J., Kerwin, J. E., and Newman, J. N. Polynomial Representation and Damping of Series 60 Hull Forms *International Shipbuilding Progress* Vol. 9, pp. 295-304, 1964.

6. Lee, C. M. *Unpublished Report in NSRDC* 1974.

7. Motora, S. and Koyama, T. Wave Excitationless Ship Forms *Sixth Symposium on Naval Hydrodynamics* pp. 383-404, 1966.

8. Newman, J. N. The Damping and Wave Resistance of a Pitching and Heaving Ship *Journal of Ship Research* Vol. 3, No. 1, pp. 1-19, 1959.

9. Newman, J. N. The Damping of an Oscillating Ellipsoid Near a Free Surface *Journal of Ship Research* Vol. 5, No. 3, pp. 44-58, 1961.

10. Newman, J. N. *Marine Hydrodynamics* Lecture Notes, Department of Ocean Engineering, M.I.T., 1971.

11. Pien, P. and Lee, C. M. Motion and Resistance of a Low-Waterplane-Area Catamaran *Ninth Symposium on Naval Hydrodynamics* 1972.

12. Tuck, E. O. A Simple 'Filon-Trapezoidal' Rule *Mathematics of Computation* Vol. 21, pp. 239-241, 1967.

13. Wehausen, J. V. and Laitone, E. V. Surface Waves *Handbuch der Physik* Vol. 9, Berlin: Springer-Verlag, 1961.

APPENDIX A

INPUT AND OUTPUT

INPUT DATA

DATA CARD 1 - FORMAT (I10, 2F10.2)

NST = The number of offset stations of the hull.

AL = Length at the waterline.

B = Half hull separation distance.

DATA CARDS 2 - FORMAT (4F10.4)

Data cards 2 consist of NST number of cards, on each of which the values of X, EPS, TO, R should be punched according to the above format.

X(I) = An array of the x-coordinates of the stations.

EPS(I) = An array of the half-beam at the waterline.

TO(I) = An array of the distance T_o. (See Fig. 5)

R(I) = An array of the radius of each section.

DATA CARD 3 - FORMAT (2I10)

NFR = The number of Froude numbers to be tested.

NOM = The number of non-dimensionalized circular frequencies to be tested.

DATA CARD(S) 4 - FORMAT (8F10.4)

FR(I) = An array of NFR number of Froude numbers.

OM(I) = An array of NOM number of the non-dimensionalized circular frequencies.

Besides the input data cards, we must supply the roots of the Legendre polynomials and the weight factors for the Gauss-Legendre quadrature in order to evaluate the semi-infinite integrals, I_2, I_4, I_5 and I_6. In the sample program, the ten-point Gauss-Legendre quadrature formula is used.

OUTPUT

Major outputs are pitch and heave damping coefficients of a single and twin hulls. However, we can get various intermediate results for checking purposes.

DP1(I) = An array of the pitch damping coefficients of a single hull.

DP2(I) = An array of the pitch damping coefficients of twin hulls.

DH1(I) = An array of the heave damping coefficients of a single hull.

DH2(I) = An array of the heave damping coefficients of twin hulls.

APPENDIX B

PROGRAM DESCRIPTIONS

Main Program

The main program handles input and output, calculates various parameters and performs six integrals in (3.8), (3.9), and (3.10) calling subroutines PIQI and ROOT. Gauss-Chebyshev quadrature formula is used for I_1 and I_3. For the rest of the integrals, the subroutine ROOT is called in order to determine the size A for the sub-integrals. (See Section 4.2.)

Subroutine PIQI

This subroutine integrates the hull function (P_i, Q_i) in (4.27) and (4.28) for a given section first and then integrates along the length of the hull. It gives the values of $\{P_i^2(K) + Q_i^2(K)\}$ for given values of K, ν, and τ.

Subroutine ZETIN

For given values of ν, τ, K and for a given section (i.e., ε, T_0, r), this subroutine evaluates the integral,

$$\gamma\nu(\tau K-1)^2 \int_{-T}^{-H} h(\xi,\zeta) e^{\nu\zeta(\tau K-1)^2} d\zeta \qquad \text{(A.1)}$$

by using Simpson's rule and returns the resulting value through the variable Z. The γ in (A.1) is the correction factor for the cylindrical part explained in Section 2.3. This subroutine is used for both (P_1, Q_1) and (P_2, Q_2).

Subroutine ZETINS

This subroutine evaluates the integral:

$$\int_{-T}^{-H} h(\xi,\zeta)\zeta e^{\nu\zeta(\tau K-1)^2} d\zeta \qquad \text{(A.2)}$$

by using Simpson's rule, which is similar to that in ZETIN. The resulting values are returned through the variable ZS which is used only for (P_1, Q_1).

Subroutine ROOT

This subroutine evaluates the zeros of $\cos\left(2\nu b\sqrt{(\tau K-1)^4 - K^2}\right) = 0$, from which we get a polynomial equation:

$$(\tau K-1)^4 - K^2 = \left(\frac{n\pi}{2\nu b}\right)^2 , \quad (n = 1,2,3,\ldots.) \qquad \text{(A.3)}$$

The roots of this polynomial are found by calling the IBM Scientific Subroutine Package POLRT. The subroutine ROOT is used in evaluating the semi-infinite integrals.

Function SS

This function calculates the submerged area of a given section. It is used in evaluating the displacement of the hull in the main program.

Function F

This function evaluates the integrand in (A.1) for the purpose of Simpson's rule.

Function S

This function evaluates the integrand in (A.2) for the purpose of Simpson's rule.

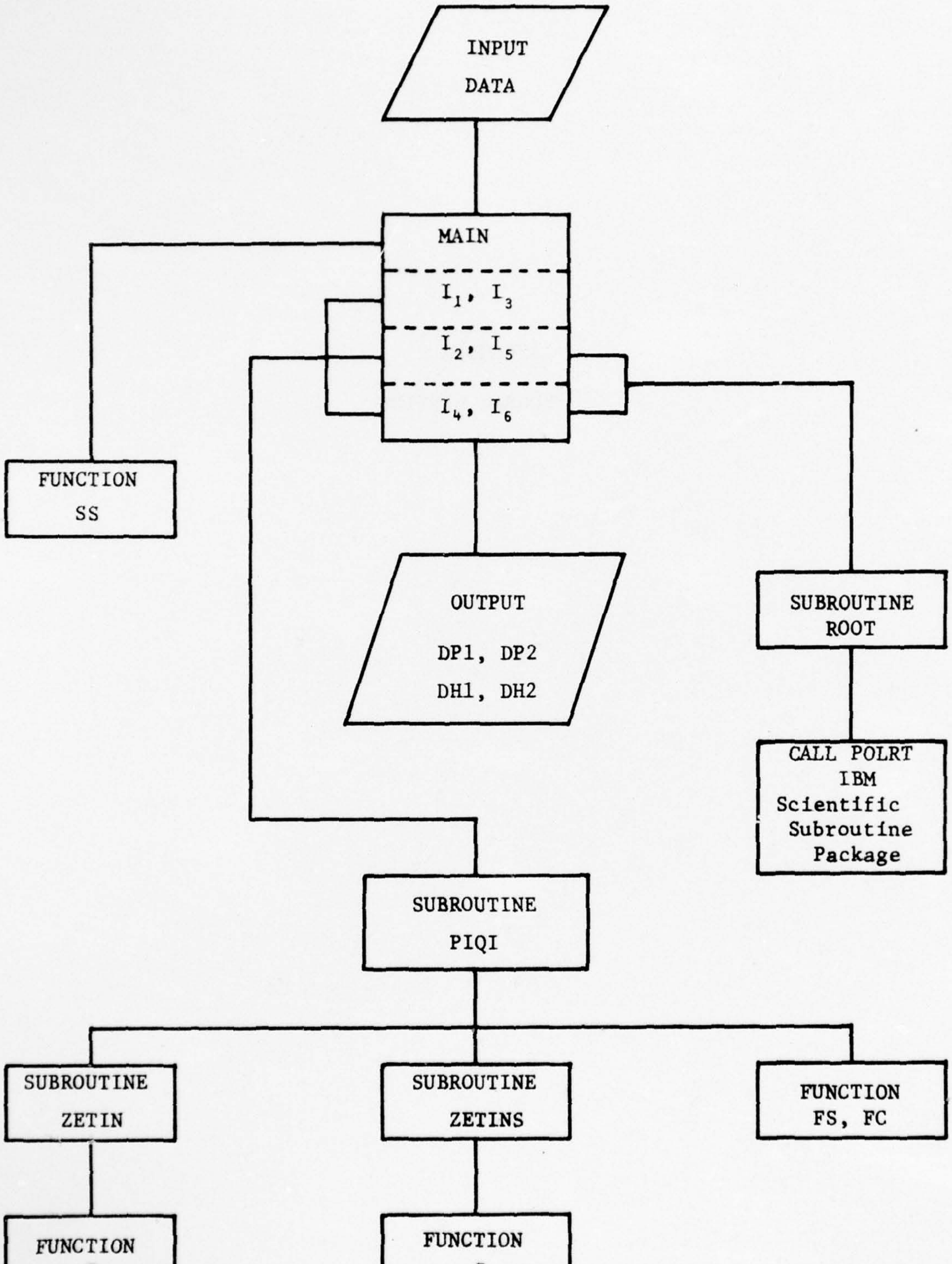

Fig. 15 Flow Chart

APPENDIX C

PROGRAM LISTING

```
C.....THIS PROGRAM COMPUTES THE PITCH AND HEAVE DAMPING COEFFICIENTS
C.....OF A SINGLE AND TWIN HULLS SWATH CONFIGURATIONS INCLUDING FORWARD
C.....SPEED EFFECTS, BASED ON NEWMAN'S THIN-SHIP THEORY.
      DIMENSION TAU(10,30),BNU(10,30)
      DIMENSION DH1(30),DH2(30),DP1(30),DP2(30)
      DIMENSION Z(10),WEIT(10)
      DIMENSION FR(10),OM(30)
C
      COMMON /GEOM/ NST,NSI,EPS(40),R(40),TO(40),X(40)
      COMMON /ONE/ ROOTR(4),ROOTI(4)
C
      DATA L/5/, M/6/
C
C.....ROOTS OF THE 10-POINT(N=9) LEGENDRE POLYNOMIALS
      Z(1)=.148874
      Z(2)=.433395
      Z(3)=.679409
      Z(4)=.865063
      Z(5)=.973906
C
C
C.....WEIGHT FACTORS FOR THE 10-POINT GAUSS-LEGENDRE QUADRATURE
      WEIT(1)=.295524
      WEIT(2)=.269266
      WEIT(3)=.219086
      WEIT(4)=.149451
      WEIT(5)=.066671
C
      DO 100 I=1,5
      J=I+5
      Z(J)=-Z(I)
      WEIT(J)=WEIT(I)
  100 CONTINUE
C
C     INPUT DATA
      READ (L,10) NST,AL,B
      WRITE(M,11) NST,AL,B
C
      READ (L,12) (X(I),EPS(I),TO(I),R(I),I=1,NST)
      WRITE(M,13) (I,X(I),EPS(I),TO(I),R(I),I=1,NST)
C
      READ (L,14) NFR,NOM
      WRITE(M,15) NFR,NOM
C
      READ (L,16) (FR(I),I=1,NFR)
      WRITE(M,17) (FR(I),I=1,NFR)
C
      READ (L,18) (OM(I),I=1,NOM)
      WRITE(M,19) (OM(I),I=1,NOM)
C
   10 FORMAT (I10,2F10.2)
   11 FORMAT (3X,'DATA:  NSRDC MODEL MODCAT 5226'//
     1          5X,'NO. OF STATIONS    =',I4/5X,
     2          'LENGTH AT THE WL  =',F7.2,' (FEET)'/
     3          5X,'HALF HULL SPACING =',F7.2,' (FEET)'////)
   12 FORMAT (4F10.4)
   13 FORMAT (5X,'STN',7X,'X(I)',7X,'EPS',7X,'TO',7X,
     1          'R'//(I7,3X,4F10.3))
   14 FORMAT (2I10)
   15 FORMAT (//5X,'NO. OF FROUDE NO. TO BE TESTED =',I3/
     1          5X,'NO. OF NON-DIM. CIRCULAR FREQ. =',I3//)
   16 FORMAT (8F10.4)
   17 FORMAT (8F10.4)
   18 FORMAT (8F10.4)
   19 FORMAT (8F10.4)
C
      NSI=NST-1
      PI=3.141592
      G=32.17
      NT=100
      NQ1=50
      NQ2=10
```

```
      WI1=PI/FLOAT(MO1)
      WI2=PI/FLOAT(MO2)
C
C     ***************************************************
C     *   CALCULATION OF THE DEMI-HULL DISPLACEMENT     *
C     *         IN CUBIC FEET FROM THE GIVEN DATA       *
C     ***************************************************
      DISP=0.
      DO 150 I=1,NST
      J=I+1
      EPS1=EPS(I)
      EPS2=EPS(J)
      R1=R(I)
      R2=R(J)
      TO1=TO(I)
      TO2=TO(J)
      X1=X(I)
      X2=X(J)
      DELX=X2-X1
      DELV=SS(EPS1,TO1,R1)+SS(EPS2,TO2,R2)
  150 DISP=DISP+DELV*DELX/2.
      WRITE(M,20) DISP
   20 FORMAT (//5X,'DISPLACEMENT =',F10.2,'(CUBIC FEET)'//)
C
C.....NON-DIMENSIONALIZING FACTORS FOR PITCH & HEAVE(SINGLE HULL)
      PNON=DISP*AL*SQRT(G*AL)
      HNON=DISP*SQRT(G/AL)
C
      DO 200 I=1,NFR
      V=SQRT(G*AL)*FR(I)
      VNOT=V/1.689
      WRITE(M,21) FR(I),V,VNOT
   21 FORMAT (//3X,'FROUDE NO=',F5.2,4X,'V(FT/S)=',F8.3,
     1           4X,'V(KNOT)=',F8.3/)
C
      DO 250 J=1,NOM
      OMEGA=OM(J)
      OMSQ=OMEGA**2*G/AL
      WN=[illegible](OMSQ)
      T=[illegible]
      XLAMDA=2.*PI*G/OMSQ
      BTAU=WN*V/G
      ANU=OMSQ/G
C
      WRITE(M,22) OMEGA,BTAU,ANU,WN,T,XLAMDA
   22 FORMAT (3X,'OMEGA(NON-DIM.)=',F6.3,4X,'TAU=',F5.2,4X,'NU=',F9.6/
     1         3X,'OMEGA(RAD/SEC.)=',F6.3,4X,'T(SEC)=',F6.3,
     2         4X,'LAMDA(FT)=',F8.2/)
C
      TAU(I,J)=BTAU
      ENU(I,J)=ANU
C
      PI1=0.
      PI2=0.
      HI1=0.
      HI2=0.
C
      IF (BTAU.EQ.0.) ITAU=1
      IF (BTAU.GT.0..AND.BTAU.LE.0.25) ITAU=2
      IF (BTAU.GT.0.25) ITAU=3
      GO TO (300,350,350), ITAU
C
C
C     ***************************************************
C     *         ZERO FORWARD SPEED CASE (TAU=0.)        *
C     *   USING MO1-POINT GAUSS-CHEBYSHEV QUADRATURE    *
C     ***************************************************
C
  300 CONTINUE
      DO 400 J1=1,MO1
      XKI=COS(FLOAT(2*J1-1)*PI/FLOAT(2*MO1))
      Z1=1.-XKI**2
```

```
      IF (Z1.LT.0.) Z1=0.
      ARG=2.*ANU*R*SQRT(Z1)
C
      CALL PIQI(XKI,ANU,BTAU,PPQ,HPQ)
C
C.....INTERMEDIATE RESULTS CAN BE PRINTED IF DESIRED
C     WRITE(M,23) XKI,ARG,PPQ,HPQ
C  23 FORMAT (2F10.4,3X,2E16.5)
C
      PPQ=-PPQ
      HPQ=-HPQ
C
      PI1=PI1+PPQ
      PI2=PI2+PPQ*2.*(COS(ARG)+1.)
      HI1=HI1+HPQ
      HI2=HI2+HPQ*2.*(COS(ARG)+1.)
  400 CONTINUE
C
      DP1(J)=((PI1*WI1)*(-2.*WN*ANU/PI))/PNON
      DH1(J)=((HI1*WI1)*(-2.*WN*ANU/PI))/HNON
      DP2(J)=((PI2*WI1)*(-WN*ANU/PI))/PNON
      DH2(J)=((HI2*WI1)*(-WN*ANU/PI))/HNON
      GO TO 410
C
  350 CONTINUE
C
C.....RK1,RK2,RK3,RK4: ROOTS OF (TAU*K-1.)**4-K**2=0.
      RK1=0.
      RK2=0.
      RK3=0.
      RK4=0.
C
C     TA1=SQRT(1.-4.*BTAU)
      TA2=SQRT(1.+4.*BTAU)
C
      TB1=2.*BTAU-1.
      TB2=2.*BTAU+1.
      TAB=2.*BTAU**2
C
      RK3=(TB2-TA2)/TAB
      RK4=(TB2+TA2)/TAB
C
      IF (ITAU.EQ.3) GO TO 500
C
      TA1=SQRT(1.-4.*BTAU)
      RK1=(TB1-TA1)/TAB
      RK2=(TB1+TA1)/TAB
  500 CONTINUE
C
      WRITE (M,27) RK1,RK2,RK3,RK4
   27 FORMAT (//5X,'K1=',E13.6,4X,'K2=',E13.6,
     1            4X,'K3=',E13.6,4X,'K4=',E13.6/)
C
      P1I2=0.
      P2I2=0.
      H1I2=0.
      H2I2=0.
C
      IF (ITAU.EQ.3) GO TO 550
C
C
C     ***************************************************
C     *  0<TAU<0.25 : FINITE INTEGRAL FROM K2 TO K3     *
C     *  USING MQ2-POINT GAUSS-CHEBYSHEV QUADRATURE     *
C     ***************************************************
C
      A1=(RK3-RK2)/2.
      B1=(RK3+RK2)/2.
C
      DO 600 J2=1,MQ2
      XKI=COS(FLOAT(2*J2-1)*PI/FLOAT(2*MQ2))
      AKI=A1*XKI+B1
```

```
C
      Z1=BTAU**2*SQRT((RK4-AKI)*(AKI-RK1))
      Z2=(BTAU*AKI-1.)**4
      Z3=Z2-AKI**2
      IF (Z3.LT.0.) Z3=0.
      Z4=COS(2.*ANU*B*SQRT(Z3))
C
      SGN=1.
      SGNX=BTAU*AKI-1.
      IF (SGNX.LT.0.) SGN=-1.
C
      ZZ1=Z2*SGN/Z1
      ZZ2=ZZ1*(2.*Z4+2.)
C
      CALL PIQI (AKI,ANU,BTAU,PPQ,HPQ)
C
      PI1=PI1+PPQ*ZZ1
      PI2=PI2+PPQ*ZZ2
      HI1=HI1+HPQ*ZZ1
      HI2=HI2+HPQ*ZZ2
  600 CONTINUE
C
      P1I2=PI1*WI2
      P2I2=PI2*WI2
      H1I2=HI1*WI2
      H2I2=HI2*WI2
C
C     ****************************************************
C     *  ITAU=2 : INTEGRATION FROM *-* INFINITY TO K1    *
C     *  ITAU=3 : INTEGRATION FROM *-* INFINITY TO K3    *
C     ****************************************************
C
  550 CONTINUE
      SUMP1=0.
      SUMP2=0.
      SUMH1=0.
      SUMH2=0.
      AA=0.
      XXX=RK1
      IF (ITAU.EQ.3) XXX=RK3
C
      DO 650 ITER=1,NI,2
C
      CALL ROOT (ITER,BTAU,ANU,B)
C
      IF (ROOTR(1).LT.XXX.AND.ROOTI(1).EQ.0.) CXX=ROOTR(1)
      IF (ROOTR(2).LT.XXX.AND.ROOTI(2).EQ.0.) CXX=ROOTR(2)
      IF (ROOTR(3).LT.XXX.AND.ROOTI(3).EQ.0.) CXX=ROOTR(3)
      IF (ROOTR(4).LT.XXX.AND.ROOTI(4).EQ.0.) CXX=ROOTR(4)
C
      BB=SQRT(XXX-CXX)
      XIN=BB-AA
C
C.....INTERMEDIATE RESULTS CAN BE PRINTED IF DESIRED
C     WRITE (M,30) ITER
C  30 FORMAT (3X,'ITER=',I3/)
C     WRITE (M,31) (ROOTR(I1),I1=1,4),(ROOTI(I1),I1=1,4)
C  31 FORMAT (8X,'R1=',E13.6,5X,'R2=',E13.6,5X,'R3=',E13.6,5X,'R4=',
C    1  E13.6/8X,'I1=',E13.6,5X,'I2=',E13.6,5X,'I3=',E13.6,5X,'I4=',
C    2  E13.6/)
C     WRITE (M,32) AA,BB,CXX
C  32 FORMAT (8X,'AA=',E13.6,4X,'BB=',E13.6,4X,'CXX=',E13.6/)
C
      PI1=0.
      PI2=0.
      HI1=0.
      HI2=0.
C
C.....10-POINT GAUSS-LEGENDRE QUADRATURE FOR A GIVEN INTERVAL
      DO 710 J3=1,10
      XKEEP=(XIN*Z(J3)+AA+BB)/2.
      WI=WEIT(J3)
```

```
      AKI=RK1-XKBAR**2
      IF (ITAU.EQ.3) AKI=RK3-XKBAR**2
      IF (ITAU.EQ.3) GO TO 710
      Z1=BTAU**2*SQRT((RK4-AKI)*(RK3-AKI)*(RK2-AKI))
      GO TO 720
  710 Z1=BTAU*SQRT(((BTAU*AKI-1.)**2+AKI)*(RK4-AKI))
  720 Z2=(BTAU*AKI-1.)**4
C
      SGN=1.
      SGNX=BTAU*AKI-1.
      IF (SGNX.LT.0.) SGN=-1.
C
      Z3=Z2-AKI**2
C     Z3 SHOULD NOT BE NEGATIVE VALUE.
C     HOWEVER, NUMERICAL ERROR MAY GIVE VERY SMALL *-* VALUE.
      IF (Z3.LT.0.) Z3=0.
      Z4=COS(2.*ANU*B*SQRT(Z3))
      ZZ1=Z2*SGN/Z1
      ZZ2=ZZ1*(2.*Z4+2.)
C
      CALL PIQI (AKI,ANU,BTAU,PPQ,HPQ)
C
      PI1=PI1+XIN*WI*PPQ*ZZ1
      PI2=PI2+XIN*WI*PPQ*ZZ2
      HI1=HI1+XIN*WI*HPQ*ZZ1
      HI2=HI2+XIN*WI*HPQ*ZZ2
  700 CONTINUE
C
      SUMP1=SUMP1+PI1
      SUMP2=SUMP2+PI2
      SUMH1=SUMH1+HI1
      SUMH2=SUMH2+HI2
C
      ERORP=ABS(PI1/SUMP1)
      ERORH=ABS(HI1/SUMH1)
C
      WRITE (M,33) PI1,SUMP1,ERORP,PI2,SUMP2
C.....INTERMEDIATE RESULTS CAN BE PRINTED IF DESIRED
C  33 FORMAT (8X,'PI1=',E13.6,4X,'SUMP1=',E13.6,4X,'ERORP=',E10.3,
C    1        4X,'PI2=',E13.6,4X,'SUMP2=',E13.6/)
C     WRITE (M,34) HI1,SUMH1,ERORH,HI2,SUMH2
C  34 FORMAT (8X,'HI1=',E13.6,4X,'SUMH1=',E13.6,4X,'ERORH=',E10.3,
C    1        4X,'HI2=',E13.6,4X,'SUMH2=',E13.6/)
C
      AA=BB
      IF (ERORP.LT.10.E-05.AND.ERORH.LT.10.E-05) GO TO 800
  650 CONTINUE
  800 CONTINUE
C
      P1I1=SUMP1
      P2I1=SUMP2
      H1I1=SUMH1
      H2I1=SUMH2
C
C     ***********************************************
C     *   TAU>0. : INTEGRATION FROM K4 TO INFINITY   *
C     ***********************************************
C
      SUMP1=0.
      SUMP2=0.
      SUMH1=0.
      SUMH2=0.
      AA=0.
C
      DO 850 ITER=1,NT,2
C
      CALL ROOT (ITER,BTAU,ANU,B)
C
      IF (ROOTR(1).GT.RK4.AND.ROOTI(1).EQ.0.) CXX=ROOTR(1)
      IF (ROOTR(2).GT.RK4.AND.ROOTI(2).EQ.0.) CXX=ROOTR(2)
      IF (ROOTR(3).GT.RK4.AND.ROOTI(3).EQ.0.) CXX=ROOTR(3)
      IF (ROOTR(4).GT.RK4.AND.ROOTI(4).EQ.0.) CXX=ROOTR(4)
```

```
C
      BE=SQRT(CXX-RK4)
      XIN=BB-AA
C
C.....INTERMEDIATE RESULTS CAN BE PRINTED IF DESIRED
C     WRITE (M,40) ITER
C  40 FORMAT (3X,'ITER=',I3/)
C     WRITE (M,41) (ROOTR(I2),I2=1,4),(ROOTI(I2),I2=1,4)
C  41 FORMAT (8X,'R1=',E13.6,5X,'R2=',E13.6,5X,'R3=',E13.6,5X,'R4=',
C    1  E13.6/8X,'I1=',E13.6,5X,'I2=',E13.6,5X,'I3=',E13.6,5X,'I4=',
C    2  E13.6/)
C     WRITE (M,42) AA,BB,CXX
C  42 FORMAT (8X,'AA=',E13.6,4X,'BB=',E13.6,4X,'CXX=',E13.6/)
C
      PI1=0.
      PI2=0.
      HI1=0.
      HI2=0.
C
C.....10-POINT GAUSS-LEGENDRE QUADRATURE FOR A GIVEN INTERVAL
      DO 900 J4=1,10
      XKBAR=(XIN*Z(J4)+AA+BB)/2.
      WI=WEIT(J4)
      AKI=RK4+XKBAR**2
      IF (ITAU.EQ.3) GO TO 910
      Z1=BTAU**2*SQRT((AKI-RK1)*(AKI-RK2)*(AKI-RK3))
      GO TO 920
  910 Z1=BTAU*SQRT(((BTAU*AKI-1.)**2+AKI)*(AKI-RK3))
  920 Z2=(BTAU*AKI-1.)**4
C
      SGN=1.
      SGNX=BTAU*AKI-1.
      IF (SGNX.LT.0.) SGN=-1.
C
      Z3=Z2-AKI**2
      IF (Z3.LT.0.) Z3=0.
      Z4=COS(2.*AND*B*SQRT(Z3))
      ZZ1=Z2*SGN/Z1
      ZZ2=ZZ1*(2.*Z4+2.)
C
      CALL FICI (AKI,AKD,BTAU,PPQ,HPQ)
C
      PI1=PI1+XIN*WI*PPQ*ZZ1
      PI2=PI2+XIN*WI*PPQ*ZZ2
      HI1=HI1+XIN*WI*HPQ*ZZ1
      HI2=HI2+XIN*WI*HPQ*ZZ2
  900 CONTINUE
C
      SUMP1=SUMP1+PI1
      SUMP2=SUMP2+PI2
      SUMH1=SUMH1+HI1
      SUMH2=SUMH2+HI2
C
      ERORP=ABS(PI1/SUMP1)
      ERORH=ABS(HI1/SUMH1)
C
C.....INTERMEDIATE RESULTS CAN BE PRINTED IF DESIRED
C     WRITE (M,50) PI1,SUMP1,ERORP,PI2,SUMP2
C  50 FORMAT (8X,'PI1=',E13.6,4X,'SUMP1=',E13.6,4X,'ERORP=',E10.3,
C    1           4X,'PI2=',E13.6,4X,'SUMP2=',E13.6/)
C     WRITE (M,51) HI1,SUMH1,ERORH,HI2,SUMH2
C  51 FORMAT (8X,'HI1=',E13.6,4X,'SUMH1=',E13.6,4X,'ERORH=',E10.3,
C    1           4X,'HI2=',E13.6,4X,'SUMH2=',E13.6/)
C
      AA=BB
      IF (ERORP.LT.10.E-05.AND.ERORH.LT.10.E-05) GO TO 950
  850 CONTINUE
  950 CONTINUE
C
      P1I3=SUMP1
      P2I3=SUMP2
      H1I3=SUMH1
```

```
      H2I3=SUMH2
C
      DP1(J)=((P1I1+P1I2+P1I3)*(-2.*WN*ANU/PI))/PNON
      DH1(J)=((H1I1+H1I2+H1I3)*(-2.*WN*ANU/PI))/HNON
      DP2(J)=((P2I1+P2I2+P2I3)*(-WN*ANU/PI))/PNON
      DH2(J)=((H2I1+H2I2+H2I3)*(-WN*ANU/PI))/HNON
C
  410 CONTINUE
  250 CONTINUE
      WRITE (M,52)  (OM(J),DP1(J),DP2(J),DH1(J),DH2(J),J=1,NOM)
   52 FORMAT (///5X,'OMEGA',10X,'DP1',13X,'DP2',13X,'DH1',13X,'DH2'//
     1        (5X,F5.3,1X,4E16.5))
  200 CONTINUE
      STOP
      END
```

```
      SUBROUTINE PIQI(AK,BNU,TAU,PPQ,HPQ)
      COMMON /GEOM/ NSI,NST,EPS(40),R(40),TO(40),X(40)
      P1=0.
      P2=0.
      Q1=0.
      Q2=0.
C
      DO 1 I=1,NSI
C.....NSI IS THE NO. OF THE INTEGRATION INTERVAL(NSI=NST-1)
      J=I+1
      EPS1=EPS(I)
      EPS2=EPS(J)
      R1=R(I)
      R2=R(J)
      TO1=TO(I)
      TO2=TO(J)
      HH1=SQRT(R1**2-EPS1**2)
      HH2=SQRT(R2**2-EPS2**2)
      H1=TO1-HH1
      H2=TO2-HH2
      X1=X(I)
      X2=X(J)
      DELX=X2-X1
      DD=BNU*(TAU*AK-1.)**2
      DDD=DD*DD
      BNUK=BNU*AK
C
      XX1=BNUK*X1
      XX2=BNUK*X2
C
      CALL ZETIN (DD,EPS1,TO1,R1,Z1)
      CALL ZETIN (DD,EPS2,TO2,R2,Z2)
C
      CALL ZETINS (DD,EPS1,TO1,R1,H1,ZS1)
      CALL ZETINS (DD,EPS2,TO2,R2,H2,ZS2)
C
```

```
      WW1=-H1*DD
      WW2=-H2*DD
C
      IF (WW1.LT.-50.) EP1=0.
      IF (WW1.LT.-50.) GO TO 10
      EP1=EXP(WW1)
C
   10 IF (WW2.LT.-50.) EP2=0.
      IF (WW2.LT.-50.) GO TO 20
      EP2=EXP(WW2)
   20 CONTINUE
C
      PH1=EPS1*EP1-Z1
      PH2=EPS2*EP2-Z2
C
      FPA1=ZS1
      FPA2=ZS2
C
      AA1=((-WW1+1.)/DDD)*EP1-(1./DDD)
      AA2=((-WW2+1.)/DDD)*EP2-(1./DDD)
      FPB1=EPS1*AA1
      FPB2=EPS2*AA2
C
      FPC1=X1*PH1
      FPC2=X2*PH2
C
      APAI=(FPA2-FPA1)/DELX
      APBI=(FPB2-FPB1)/DELX
      APCI=(FPC2-FPC1)/DELX
C
      BPAI=FPA1-APAI*X1
      BPBI=FPB1-APBI*X1
      BPCI=FPC1-APCI*X1
C
      IF (BNUK.EQ.0.) GO TO 50
C
      FFS1=(FC(XX2)-FC(XX1))/BNUK
      FFC1=(FS(XX2)-FS(XX1))/BNUK
C
      FSS1=SIN(XX2)-SIN(XX1)
      FCC1=COS(XX1)-COS(XX2)
C
      FFS2=(FS(XX2)-FS(XX1))/BNUK**2
      FFC2=(FC(XX2)-FC(XX1))/BNUK**2
C
      FSS2=(COS(XX1)-COS(XX2))/BNUK
      FCC2=(SIN(XX2)-SIN(XX1))/BNUK
C
      AHI=(PH2-PH1)/DELX
      BHI=PH1-AHI*X1
C
      PP1=-((APAI+APBI)*FFS1+(BPAI+BPBI)*FSS1)
     1    -(APCI*FFS2+BPCI*FSS2)
      QQ1= (APAI+APBI)*FFC1+(BPAI+BPBI)*FCC1
     1    -(APCI*FFC2+BPCI*FCC2)
      PP2=AHI*FFS2+BHI*FSS2
      QQ2=AHI*FFC2+BHI*FCC2
C
      P1=P1+PP1
      Q1=Q1+QQ1
      P2=P2+PP2
      Q2=Q2+QQ2
C
      GO TO 1
   50 CONTINUE
C
C.....CASE FOR BNUK=0.
C     P1=P2=0.
      Q1=Q1-(FPC1+FPC2)*DELX/2.
      Q2=Q2+(PH1+PH2)*DELX/2.
C
    1 CONTINUE
```

```
C                                                                       PIQI0109
      PEQ=P1**2+Q1**2                                                   PIQI0110
      HEQ=P2**2+Q2**2                                                   PIQI0111
C                                                                       PIQI0112
      RETURN                                                            PIQI0113
      END                                                               PIQI0114



      SUBROUTINE ZETIN(DD,EPS,T,R,Z)                                    ZETN0001
      IF(R.EQ.0.) Z=0.                                                  ZETN0002
      IF(R.EQ.0.) RETURN                                                ZETN0003
      NUM=10                                                            ZETN0004
      DIV=2.*FLOAT(NUM)                                                 ZETN0005
      A=EPS/R                                                           ZETN0006
      GAMMA=2.                                                          ZETN0007
      ALPA=ASIN(A)                                                      ZETN0008
      B=R*COS(ALPA)                                                     ZETN0009
      TA=B-T                                                            ZETN0010
      TB=-T-B                                                           ZETN0011
C.... R,T ARE POSITIVE ( THE RADIOUS AND DEPTH TO THE AXIS)             ZETN0012
      H=(TA-TB)/DIV                                                     ZETN0013
      X=TB                                                              ZETN0014
      Z=0.                                                              ZETN0015
      DO 1 I=1,NUM                                                      ZETN0016
      XH=X+H                                                            ZETN0017
      XHH=X+2.*H                                                        ZETN0018
      Z=Z+H/3.*(F(DD,T,R,X)+4.*F(DD,T,R,XH)+F(DD,T,R,XHH))              ZETN0019
    1 X=X+2.*H                                                          ZETN0020
      Z=GAMMA*Z*DD                                                      ZETN0021
      RETURN                                                            ZETN0022
      END                                                               ZETN0023



      SUBROUTINE ZETINS (DD,EES,TO,R,H,ZS)                              ZTNS0001
C     DD=NU*(TAU*K-1)**2                                                ZTNS0002
      IF (R.EQ.0.) ZS=0.                                                ZTNS0003
      IF (R.EQ.0.) RETURN                                               ZTNS0004
      N=10                                                              ZTNS0005
      DIV=2.*FLOAT(N)                                                   ZTNS0006
      T=TO+R                                                            ZTNS0007
      B=(T-H)/DIV                                                       ZTNS0008
C.....'B' IS THE SPACING OF THE INTEGRATION                             ZTNS0009
      X=-T                                                              ZTNS0010
      ZS=0.                                                             ZTNS0011
C                                                                       ZTNS0012
      DO 1 I=1,N                                                        ZTNS0013
      XB=X+B                                                            ZTNS0014
      XBB=X+2.*B                                                        ZTNS0015
      ZS=ZS+B/3.*(S(DD,TO,R,X)+4.*S(DD,TO,R,XB)+S(DD,TO,R,XBB))         ZTNS0016
    1 X=X+2.*B                                                          ZTNS0017
C                                                                       ZTNS0018
      RETURN                                                            ZTNS0019
      END                                                               ZTNS0020
```

```
      SUBROUTINE ROOT(ITER,TAU,ANU,YDIS)
      DIMENSION XCOF(5),COF(5)
      COMMON/ONE/ROOTR(4),ROOTI(4)
      MM=4
      PI=3.14159
      XPI=PI*FLOAT(ITER)
      A=-4./TAU
      B=6./TAU**2-1./TAU**4
      C=-4./TAU**3
      DD=XPI/(2.*ANU*YDIS)
      D=(1.-DD*DD)/TAU**4
      XCOF(1)=D
      XCOF(2)=C
      XCOF(3)=B
      XCOF(4)=A
      XCOF(5)=1.
      CALL POLRT(XCOF,COF,MM,ROOTR,ROOTI,IER)
      RETURN
      END
```

```
      FUNCTION F(D,T,R,X)
      A=T+X
      AA=A*A
      EE=R*R-AA
      EE=ABS(EE)
      B=SQRT(EE)
      A1=D*X
      A2=-A1
      IF(A2.GT.50.) F=0.
      IF(A2.GT.50.) RETURN
      F=B*EXP(A1)
      RETURN
      END
      FUNCTION S(DD,TO,R,ZETA)
      A=ZETA+TO
      ARG=ABS(R*R-A*A)
C.....'R' IS LESS THAN OR EQAL TO 'A', BUT DUE TO THE SLIGHT
C.....NUMERICAL ERROR, R*R-A*A SOMETIMES GIVES '-' VALUES, THUS
C.....TAKING THE ABS(R*R-A*A) IS PREFERRED.
      H=SQRT(ARG)
      AA=DD*ZETA
C
      IF (AA.LT.-50.) S=0.
      IF (AA.LT.-50.) RETURN
C
      S=H*ZETA*EXP(AA)
      RETURN
      END
```

```
      FUNCTION FS(X)
      A=SIN(X)
      B=X*COS(X)
      FS=A-B
      RETURN
      END
      FUNCTION FC(X)
      A=COS(X)
      B=X*SIN(X)
      FC=A+B
      RETURN
      END
      FUNCTION SS(EPS,TO,RO)
      PI=3.1415926
      IF(RO.EQ.0.) SS=0.
      IF(RO.EQ.0.) RETURN
      ALPA=ASIN(EPS/RO)
      B=RO*COS(ALPA)
      BB=B/2.
      A1=2.*EPS*(TO-BB)
      A2=RO**2*(PI-ALPA)
      SS=A1+A2
      RETURN
      END
      FUNCTION ASIN(X)
      A=SQRT(1.-X*X)
      B=X/A
      ASIN=ATAN(B)
      RETURN
      END
```

November 1973

DISTRIBUTION LIST FOR UNCLASSIFIED
TECHNICAL REPORTS ISSUED UNDER
CONTRACT N00014-67-A-0204-0023 TASK NR 062-411

All addressees receive one copy unless otherwise specified

Defense Documentation Center
Cameron Station
Alexandria, VA 22314 **12 copies**

Technical Library
Naval Ship Research & Dev. Center
Annapolis Laboratory
Annapolis, MD 21402

Professor Bruce Johnson
Engineering Department
Naval Academy
Annapolis, MD 21402

Library
Naval Academy
Annapolis, MD 21402

Professor C. S. Yih
Department of Engineering Mechanics
University of Michigan
Ann Arbor, MI 48108

Professor W. P. Graebel
Department of Engineering Mechanics
University of Michigan
Ann Arbor, MI 48108

Professor T. Francis Ogilvie
Department of Naval Architecture
and Marine Engineering
University of Michigan
Ann Arbor, MI 48108

Professor W. W. Willmarth
Department of Aerospace Engineering
University of Michigan
Ann Arbor, MI 48108

Professor R. B. Couch
Department of Naval Architecture
and Marine Engineering
University of Michigan
Ann Arbor, MI 48108

Air Force Office of Scientific
Research (REM)
1400 Wilson Boulevard
Arlington, VA 22209

Dr. Coda Pan
Shaker Research Corporation
Northway 10 Executive Park
Ballston Lake, NY 12019

Professor S. Corrsin
Department of Mechanics and
Materials Sciences
The Johns Hopkins University
Charles and 34th Street
Baltimore, MD 21218

Professor L. S. G. Kovasznay
Department of Mechanics and Materials
Sciences
The Johns Hopkins University
Charles and 34th Street
Baltimore, MD 21218

Professor O. M. Phillips
Department of Earth and Planetary
Sciences
The Johns Hopkins University
Charles and 34th Street
Baltimore, MD 21218

Professor M. Holt
Department of Mechanical Engineering
University of California
Berkeley, CA 94720

Professor E. V. Laitone
Department of Mechanical Engineering
University of California
Berkeley, CA 94720

Librarian
Department of Naval Architecture
University of California
Berkeley, CA 94720

Professor P. Lieber
Department of Mechanical Engineering
University of California
Berkeley, CA 94720

Professor J. R. Paulling
Department of Naval Architecture
University of California
Berkeley, CA 94720

Professor W. C. Webster
Department of Naval Architecture
University of California
Berkeley, CA 94720

Professor J. V. Wehausen
Department of Naval Architecture
University of California
Berkeley, CA 94720

Professor J. A. Schetz
Department of Aerospace Engineering
Virginia Polytechnic Institute
Blacksburg, VA 24061

Director
Office of Naval Research Branch Office
495 Summer Street
Boston, MA 02210

Commander
Boston Naval Shipyard
Boston, MA 02129

Commander
Puget Sound Naval Shipyard
Bremerton, WA 98314

Dr. Alfred Ritter
[illegible]
[illegible]
Buffalo, NY 14221

Professor G. Birkhoff
Department of Mathematics
Harvard University
Cambridge, MA 02138

Professor G. F. Carrier
Division of Engineering and
Applied Physics
Pierce Hall
Harvard University
Cambridge, MA 02138

Commanding Officer
NROTC Naval Administrative Unit
Massachusetts Institute of Technology
Cambridge, MA 02139

Professor M. A. Abkowitz
Department of Ocean Engineering
Massachusetts Institute of Technology
Cambridge, MA 02139

Professor C. C. Mei
Department of Civil Engineering
Massachusetts Institute of Technology
Cambridge, MA 02139

Professor Phillip Mandel
Department of Ocean Engineering
Massachusetts Institute of Technology
Cambridge, MA 02139

Professor E. W. Merrill
Department of Chemical Engineering
Massachusetts Institute of Technology
Cambridge, MA 02139

Professor L. N. Howard
Department of Mathematics
Massachusetts Institute of Technology
Cambridge, MA 02139

Professor R. F. Probstein
Department of Mechanical Engineering
Massachusetts Institute of Technology
Cambridge, MA 02139

Professor E. Mollo-Christensen
Department of Meteorology
Room 54-1722
Massachusetts Institute of Technology
[illegible]

Professor J. Nicholas Newman
Department of Ocean Engineering
Room 5-324A
Massachusetts Institute of Technology
Cambridge, MA 02139

Professor A. R. Kuhlthau, Director
Research Laboratories for the Engineering
Sciences
Thornton Hall
University of Virginia
Charlottesville, VA 22903

Director
Office of Naval Research Branch Office
536 South Clark Street
Chicago, IL 60605

Library
Naval Weapons Center
China Lake, CA 93555

Institute of Hydrodynamics and Hydraulic
Engineering
Technical University of Denmark
Building 115 DK-2800
Lyngby/Copenhagen, Denmark

Page 3

Professor E. Reshotko
Division of Chemical Engineering
Science
Case Western Reserve University
Cleveland, OH 44106

Professor J. M. Burgers
Institute of Fluid Dynamics and
Applied Mathematics
University of Maryland
College Park, MD 20742

Professor Pai
Institute for Fluid Dynamics and
Applied Mathematics
University of Maryland
College Park, MD 20740

Acquisitions Branch (S-AK/DL)
NASA Scientific and Technical
Information Facility
P. O. Box 33
College Park, MD 20740

Technical Library
Naval Weapons Laboratory
Dahlgren, VA 22448

Computation & Analyses Laboratory
Naval Weapons Laboratory
Dahlgren, VA 22448

Dr. C. S. Wells, Jr.
Advanced Technology Center, Inc.
P. O. Box 6144
Dallas, TX 75222

Dr. R. H. Kraichnan
Dublin, NH 03444

Army Research Office
Box CM, Duke Station
Durham, NC 27706

Dr. Martin H. Bloom
Polytechnic Institute of New York
Department of Aerospace Engineering
and Applied Mechanics
Farmingdale, NY 11735

Technical Documents Center
Army Mobility Equipment R&D Center
Fort Belvoir, VA 22060

Professor J. E. Cermak
Department of Civil Engineering
Fluid Mechanics Program
Colorado State University
Fort Collins, CO 80521

Professor O. H. Shemdin
Coastal and Oceanographic Engineering
Department
University of Florida
Gainesville, FL 32601

Technical Library
Webb Institute of Naval Architecture
Glen Cove, NY 11542

Professor E. V. Lewis
Webb Institute of Naval Architecture
Glen Cove, NY 11542

Dr. M. Poreh
Technion-Israel Institute of Technology
Department of Civil Engineering
Haifa, Israel

Dr. J. P. Breslin
Davidson Laboratory
Stevens Institute of Technology
Castle Point Station
Hoboken, NJ 07030

Mr. C. H. Henry
Stevens Institute of Technology
Davidson Laboratory
Castle Point Station
Hoboken, NJ 07030

Dr. D. Savitsky
Davidson Laboratory
Stevens Institute of Technology
Castle Point Station
Hoboken, NJ 07030

Dr. A. Strumpf
Davidson Laboratory
Stevens Institute of Technology
Castle Point Station
Hoboken, NJ 07030

Dr. J. P. Craven
University of Hawaii
1801 University Avenue
Honolulu, HI 96822

Page 4

Professor F. Hussain
Department of Mechanical Engineering
Cullen College of Engineering
University of Houston
Houston, TX 77004

Professor J. F. Kennedy, Director
Institute of Hydraulic Research
University of Iowa
Iowa City, IA 52242

Professor L. Landweber
Institute of Hydraulic Research
University of Iowa
Iowa City, IA 52242

Professor E. L. Resler
Graduate School of Aerospace Engineering
Cornell University
Ithaca, NY 14850

Dr. D. E. Ordway
Sage Action, Incorporated
P. O. Box 416
Ithaca, NY 14850

Dr. S. A. Orszag
Flow Research, Inc.
1819 South Central Avenue
Suite 72
Kent, WA 98031

Professor J. W. Miles
Institute of Geophysics and
Planetary Physics
University of California, San Diego
La Jolla, CA 92037

Director
Scripps Institute of Oceanography
University of California
La Jolla, CA 92037

Professor A. T. Ellis
Department of Applied Mathematics and
Engineering Sciences
University of California, San Diego
La Jolla, CA 92037

Dr. J. Young
Science Applications, Incorporated
1250 Prospect Street
La Jolla, CA 92037

Mr. Phillip Eisenberg, President
Hydronautics, Incorporated
7210 Pindell School Road
Laurel, MD 20810

Mr. M. P. Tulin
Hydronautics, Incorporated
7210 Pindell School Road
Laurel, MD 20810

Commander
Long Beach Naval Shipyard
Long Beach, CA 90801

Dr. C. W. Hirt
University of California
Los Alamos Scientific Laboratory
P. O. Box 1663
Los Alamos, NM 87544

Professor John Laufer
Department of Aerospace Engineering
University of Southern California
University Park
Los Angeles, CA 90007

Professor J. M. Killen
St. Anthony Falls Hydraulic Laboratory
University of Minnesota
Minneapolis, MN 55414

Lorenz G. Straub Library
St. Anthony Falls Hydraulic Laboratory
University of Minnesota
Minneapolis, MN 55414

Professor J. Ripkin
St. Anthony Falls Hydraulic Laboratory
University of Minnesota
Minneapolis, MN 55414

Dr. E. Silberman
St. Anthony Falls Hydraulic Laboratory
University of Minnesota
Minneapolis, MN 55414

Library
Naval Postgraduate School
Monterey, CA 93940

Professor A. B. Metzner
Department of Chemical Engineering
University of Delaware
Newark, NJ 19711

Page 5

Technical Library
Naval Underwater Systems Center
Newport, RI 02840

Office of Naval Research
New York Area Office
207 W. 24th Street
New York, NY 10011

Professor V. Castelli
Department of Mechanical Engineering
Columbia University
New York, NY 10027

Professor H. G. Elrod
Department of Mechanical Engineering
Columbia University
New York, NY 10027

Engineering Societies Library
345 East 47th Street
New York, NY 10017

Professor J. J. Stoker
Courant Institute of Mathematical Sciences
New York University
251 Mercer Street
New York, NY 10003

Society of Naval Architects and Marine Engineers
74 Trinity Place
New York, NY 10006

Librarian, Aeronautical Laboratory
National Research Council
Montreal Road
Ottawa 7, Canada

Technical Library
Naval Coastal System Laboratory
Panama City, FL 32401

Dr. Jack W. Hoyt
Code 2501
Naval Undersea Center
San Diego, CA 92132

Technical Library
Naval Undersea Center
Pasadena Laboratory
3202 E. Foothill Blvd.
Pasadena, CA 91107

Professor A. J. Acosta
Department of Mechanical Engineering
California Institute of Technology
Pasadena, CA 91109

Professor H. W. Liepmann
Graduate Aeronautical Laboratories
California Institute of Technology
Pasadena, CA 91109

Professor M. S. Plesset
Engineering Science Department
California Institute of Technology
Pasadena, CA 91109

Professor A. Roshko
Graduate Aeronautical Laboratories
California Institute of Technology
Pasadena, CA 91109

Professor T. Y. Wu
Engineering Science Department
California Institute of Technology
Pasadena, CA 91109

Director
Office of Naval Research Branch Office
1030 E. Green Street
Pasadena, CA 91101

Professor K. M. Agrawal
Virginia State College
Department of Mathematics
Petersburg, VA 23803

Technical Library
Naval Ship Engineering Center
Philadelphia Division
Philadelphia, PA 19112

Technical Library
Philadelphia Naval Shipyard
Philadelphia, PA 19112

Professor R. C. MacCamy
Department of Mathematics
Carnegie Institute of Technology
Pittsburgh, PA 15213

Dr. Paul Kaplan
Oceanics, Inc.
Technical Industrial Park
Plainview, NY 11803

Page 6

Technical Library
Naval Missile Center
Point Mugu, CA 93041

Commander
Portsmouth Naval Shipyard
Portsmouth, NH 03801

Commander
Norfolk Naval Shipyard
Portsmouth, VA 23709

Dr. H. Norman Abramson
Southwest Research Institute
8500 Culebra Road
San Antonio, TX 78228

Editor
Applied Mechanics Review
Southwest Research Institute
8500 Culebra Road
San Antonio, TX 78206

Dr. Andrew Fabula
Code 600, Building 106
Naval Undersea Center
San Diego, CA 92132

Office of Naval Research
San Francisco Area Office
760 Market Street, Room 447
San Francisco, CA 94102

Library
Pearl Harbor Naval Shipyard
Box 400
FPO San Francisco 96610

Technical Library
Hunters Point Naval Shipyard
San Francisco, CA 94135

Professor C. E. Pearson
Aerospace Research Laboratory
University of Washington
Seattle, WA 98105

Professor Bruce H. Adee
Department of Mechanical Engineering
University of Washington
Seattle, WA 98195

Professor A. Hertzberg
Director, Aerospace Research Laboratory
University of Washington
Seattle, WA 98105

Fenton Kennedy Document Library
The Johns Hopkins University
Applied Physics Laboratory
8621 Georgia Avenue
Silver Spring, MD 20910

Professor E. Y. Hsu
Department of Civil Engineering
Stanford University
Stanford, CA 94305

Dr. Byrne Perry
Department of Civil Engineering
Stanford University
Stanford, CA 94305

Dr. R. L. Street
Department of Civil Engineering
Stanford University
Stanford, CA 94305

Professor Milton van Dyke
Department of Aeronautical Engineering
Stanford University
Stanford, CA 94305

Professor R. Pfeffer
Geophysical Fluid Dynamics Institute
Florida State University
Tallahassee, FL 32306

Professor R. C. DiPrima
Department of Mathematics
Rensselaer Polytechnic Institute
Troy, NY 12181

Dr. L. A. Segel
Department of Mathematics
Rensselaer Polytechnic Institute
Troy, NY 12181

Professor J. W. Holl
The Pennsylvania State University
Department of Aerospace Engineering
University Park, PA 16801

Page 7

Professor J. L. Lumley
Department of Aerospace Engineering
Pennsylvania State University
University Park, PA 16802

Dr. J. M. Robertson
Department of Theoretical and
Applied Mechanics
University of Illinois
Urbana, IL 61803

Technical Library
Mare Island Naval Shipyard
Vallejo, CA 94592

Mr. Norman Nilsen(SP 2022)
Strategic Systems Project
Office
Department of the Navy
Washington, DC 20376

Office of Naval Research
Code 438
800 N. Quincy Street
Arlington, VA 22217 (3) copies

Office of Naval Research
Code 411-7
800 N. Quincy Street
Arlington, VA 22217

Office of Naval Research
Code 411-6
800 N. Quincy Street
Arlington, VA 22217

Office of Naval Research
Code 412-8
800 N. Quincy Street
Arlington, VA 22217

Office of Naval Research
Code 412-3
800 N. Quincy Street
Arlington, VA 22217

Office of Naval Research
Code 473
800 N. Quincy Street
Arlington, VA 22217

Office of Naval Research
Code 481
800 N. Quincy Street
Arlington, VA 22217

Naval Research Laboratory
Code 2627
Washington, DC 20375 (6) copies

Naval Research Laboratory
Code 2629 (ONRL)
Washington, DC 20375 (6) copies

Naval Research Laboratory
Code 6170
Washington, DC 20375

Naval Research Laboratory
Code 4000
Washington, DC 20375

Naval Research Laboratory
Code 8030
Washington, DC 20375

Naval Research Laboratory
Code 8040
Washington, DC 20375

Naval Ship Systems Command
Code 031
Washington, DC 20362

Naval Ship Systems Command
Code 0341
Washington, DC 20362

Naval Sea Systems Command
Code 0322 (L. Benen)
Washington, DC 20362

Naval Sea Systems Command
Code 032 (J. Schuler)
Washington, DC 20362

Naval Sea Systems Command
Code 09GS (Library)
Washington, DC 20362

Page 8

Naval Ship Engineering Center
Code 6034
Center Building
Prince George's Center
Hyattsville, MD 20782

Naval Ship Engineering Center
Code 6101E
Center Building
Prince George's Center
Hyattsville, MD 20782

Naval Ship Engineering Center
Code 6110
Center Building
Prince George's Center
Hyattsville, MD 20782

Naval Ship Engineering Center
Code 6114
Center Building
Prince George's Center
Hyattsville, MD 20782

Naval Ship Engineering Center
Code 6136
Center Building
Prince George's Center
Hyattsville, MD 20782

Dr. A. Powell (Code 01)
Naval Ship Research & Dev. Center
Bethesda, MD 20034

Mr. W. M. Ellsworth (Code 11)
Naval Ship Research & Dev. Center
Bethesda, MD 20034

Dr. W. E. Cummins (Code 15)
Naval Ship Research & Dev. Center
Bethesda, MD 20034

Mr. G. H. Gleissner (Code 18)
Naval Ship Research & Dev. Center
Bethesda, MD 20034

Mr. R. Wermter (Code 152)
Naval Ship Research & Dev. Center
Bethesda, MD 20034

Dr. W. B. Morgan (Code 154)
Naval Ship Research & Dev. Center
Bethesda, MD 20034

Mr. J. B. Hadler (Code 156)
Naval Ship Research & Dev. Center
Bethesda, MD 20034

Library (Code 5641)
Naval Ship Research & Dev. Center
Bethesda, MD 20034

Dr. P. Pien (Code 1521)
Naval Ship Research & Dev. Center
Bethesda, MD 20034

Mr. Paul S. Granville (Code 1541)
Naval Ship Research & Dev. Center
Bethesda, MD 20034

Mr. J. McCarthy (Code 1552)
Naval Ship Research & Dev. Center
Bethesda, MD 20034

Dr. Nils Salvesen (Code 1552)
Naval Ship Research & Dev. Center
Bethesda, MD 20034

Ms. Joanna Schot (Code 1843)
Naval Ship Research & Dev. Center
Bethesda, MD 20034

Dr. M. Strasberg (Code 1901)
Naval Ship Research & Dev. Center
Bethesda, MD 20034

Naval Air Systems Command
AIR 03
Washington, DC 20361

Naval Air Systems Command
AIR 5301
Washington, DC 20361

Naval Air Systems Command
AIR 50174
Washington, DC 20361

Naval Ordnance Systems Command
ORD 03A
Washington, DC 20360

Naval Sea Systems Command
Code 03512 (T. Peirce)
Washington, D. C. 20362

Naval Ordnance Systems Command
ORD 5413
Washington, DC 20360

Strategic Systems Project Office
CNM (PM-1)
Washington, DC 20360

Oceanographer of the Navy
200 Stovall Street
Alexandria, VA 22332

Commander
Naval Oceanographic Office
Washington, DC 20373

Dr. A. L. Slafkosky
Scientific Advisor
Commandant of the Marine Corps
(Code AX)
Washington, DC 20380

Librarian Station 5-2
Coast Guard Headquarters
NASSIF Building
400 Seventh Street, S.W.
Washington, DC 20591

Office of Research and Development
Maritime Administration
441 G Street, N.W.
Washington, DC 20235

Division of Ship Design
Maritime Administration
441 G Street, N.W.
Washington, DC 20235

National Science Foundation
Engineering Division
1800 G Street, N.W.
Washington, DC 20550

Dr. G. Kulin
Fluid Mechanics Section
National Bureau of Standards
Washington, DC 20234

Science & Technology Division
Library of Congress
Washington, DC 20540

Chief of Research and Development
Office of Chief of Staff
Department of the Army
Washington, DC 20310

Professor A. Thiruvengadam
Department of Mechanical Engineering
Catholic University of America
Washington, DC 20017

Librarian
Naval Ordnance Laboratory
White Oak, MD 20910

Mr. J. Enig (Room 3-252)
Naval Ordnance Laboratory
White Oak, MD 20910

Dr. A. S. Iberall, President
General Technical Services, Inc.
451 Penn Street
Yeadon, PA 19050